

"Dissemination of Education for Knowledge Science and Culture"
-Shikshanmaharshi Dr. Bapuji Salunkhe

Shri Swami Vivekanand Shikshan Sanstha's

Vivekanand College (Autonomous), Kolhapur

Department of Physics

M.Sc. II (2022-23)

Research Project Title

Roll.No.	Name of Students	Name of Guide	Title of Project
1332	Chougule Shraddha Sanjay	Dr. S. S. Latthe	Camphour Soot Based Superhydrophobic coating on marble by self-cleaning application
1334	Gaikwad Aishwarya Suryakant	Prof. A. V. Shinde	Synthesis and Characterization of ZnO by CBD
1335	Gaikwad Divya Ramesh	Dr. S. S. Latthe	Fabrication of Superhydrophobic Polycarbonate substrate by using Template method
1336	Gawade Sayli Shantaram	Dr. S. S. Latthe	Fabrication of Superhydrophobic Polycarbonate substrate by using Template method
1337	Gurav Rutuja Ravindra	Prof. A. V. Shinde	Synthesis & Characterization of ZnO nanoparticles by CBD
1338	Hirave Pravin Prakash	Prof. A. V. Shinde	Deposition by thin film by Silar method
1339	Jadhav Nikhil Sandeep	Dr. S. S. Latthe	Superhydrophobic coating from Camphor soot PMMP for Selfcleaning
1340	Jamadar Wahida Sardar	Dr. S. S. Latthe	Superhydrophobic coating from Camphor soot Nanoparticles for Selfcleaning
1341	Kakde Semma Vishnu	Prof. A. V. Shinde	Preparation of ZnO thin film by CBD



1342	Khandekar Pooja Sanjay	Prof. A. V. Shinde	Introduction of Thin Film CuO by CBD
1343	Khokar Raeez Rafiq	Prof. A. V. Shinde	Synthesis & Characterization of ZnO nanoparticles by CBD
1344	Khot Priyanka Balaso	Dr. S. S. Latthe	Fabrication of SHP polycarbonate substance by template method
1345	Koli Sayli Santosh	Prof. A. V. Shinde	Preparation of ZnO thin film by CBD
1346	Kondare Adinath Bhaskar	Prof. A. V. Shinde	Preparation of MnSO ₄ thin film by CBD
1347	Kore Jyoti Vinayak	Dr. S. I. Inamdar	X- Ray Diffraction
1348	Kshirsagar Vijaya Suresh	Dr. S. S. Latthe	Candel soot-based SHP coatings for oil- water separation
1349	Kumbhar Pooja Prakash	Prof. A. V. Shinde	Synthesis & Characterization of ZnO nanoparticle by CBD method
1350	Kurade Shubhangi Shivaji	Prof. A. V. Shinde	Theoretical study of thin film deposition-based supercapacitor & characterization
1351	Latthe Sammer Rajendra	Dr. S. S. Latthe	Fabrication of SHP coating by camphor/ polystyrene composite for self-cleaning
1352	Nikam Mrunali Tanaji	Dr. S. S. Latthe	Candel soot-based SHP coatings on sponge by self-cleaning application
1353	Patil Aakansha Bhimrao	Dr. S. I. Inamdar	X- Ray Diffraction
1354	Patil Anuja Dattajirao	Prof. A. V. Shinde	Deposition of CdS thin film by CBD method
1355	Patil Rajat Jaywant	Dr. S. I. Inamdar	Synthesis & Characterization of ZnFe by microwave auto combustion method
	Patil Sanyogita Sanjay	Dr. S. S. Latthe	Candle Soot based SHP coatings on sponge by self-cleaning application



1357	Patil Shrutika Jaysing	Prof. A. V. Shinde	Preparation of ZnO thin film by CBD
1358	Pirale Siddhant Deepak	Prof. A. V. Shinde	Preparation of Fe ₂ O ₃ thin film by SILAR
1359	Rajguru Supriya Dhanaji	Dr. S. I. Inamdar	Preparation of Cobalt Zinc Ferrite by microwave method
1360	Rajput Prerana Pundlik	Dr. S. S. Latthe	Camphour Soot Based Superhydrophobic coating on marble by self-cleaning application
1361	Sakate Santosh Shripati	Prof. A. V. Shinde	Preparation of ZnO thin film by CBD
1363	Shelar Avinash Sanjay	Prof. A. V. Shinde	Preparation of Cobalt Zinc Ferrite by microwave auto combustion
1364	Sonkamble Rohan Raju	Dr. S. I. Inamdar	X- Ray Diffraction
1365	Sutar Pooja Vishwanath	Dr. S. S. Latthe	Camphour Soot Based Superhydrophobic coating on marble by self-cleaning application

A. Kamble

M.Sc. Co-ordinator

Dr. S. I. Inamdar

Head

Department of Physics

**Head of the
Department of Physics
Vivekanand College, Kolhapur**



Candle Soot Based on Superhydrophobic Surfaces Coating on sponge by oil-waterseperation

A Dissertation Report Submitted to

Vivekanand College, Kolhapur (Autonomous)

For the partial fulfillment of

Degree of Master of science

In

PHYSICS

Under the Faculty of Science

by

Miss. Mrunali Tanaji Nikam

(B.Sc)

Under the Guidance of

Dr. S. S. Latthe

(M.sc Ph.D.)

Department of Physics

Vivekanand College, Kolhapur

(Autonomous)

2022-2023



DECLARATION

I hereby declare that, the project entitled " **Candle soot based on superhydrophobic surfaces on sponges for oil-water separation**" completed and written by me has not previously Formed the basis for the award of any Degree or Diploma or Other similar title of this or any other university or examining body.

Place: Kolhapur

Date: 26/05/2023



Miss. Mrunali Tanaji Nikam (B.Sc)

Department of Physics

Vivekanand College, Kolhapur

(Autonomous)

2022-2023



CERTIFICATE

This is to certify that the project entitled " **Candle soot based on superhydrophobic surfaces on sponges for oil-water separation**" which is being submitted herewith for the award of the Degree of **Master of Science in Physics** of **Vivekanand College, Kolhapur (Autonomous)**, is the result of the original project work completed by **Miss. Mrunali Tanaji Nikam (B.Sc)** ,under our supervision and guidance and to the best of our knowledge and belief the work embodied in this project has not formed earlier the basis for the award of any degree or similar titled of this or any other university or examining body.

Place: Kolhapur


Date:



Dr. S.S. Latthe

M.Sc Ph. D

Project Guide



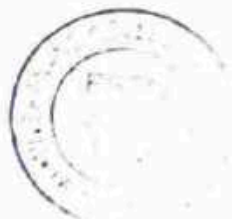
Examiner



Dr. C. J. Kamble

Head of Department

HEAD
DEPARTMENT OF PHYSICS
VIVEKANAND COLLEGE, KOLHAPUR
(AUTONOMOUS)



Acknowledgement

On the day of completion of this project, I offer sincere gratitude to those who encouraged and helped me a lot at various stages of this work.

I have great pleasure to express my deep sense of indebtedness and heart full gratitude to Dr.S.S.Latthe, Professor, Department of Physics, Vivekanand College (Autonomous), Kolhapur, for his expert and valuable guidance and continuous encouragement given to me during the course of my project work. He has already been a source of strength for me. I find in him a real researcher who through his own example and devotion for scientific work inspired me towards a common goal of achieving scientific knowledge and pursuit.

I wish to express my appreciation to Prof. S.V. Malgaonkar, Prof. C.J. Kamble, Prof. G.J. Navathe, Prof. Inamdar for discussion and co-operation in each and every movement of my project work.

My acknowledgement will be incomplete if I don't express my appreciation towards my family members whose good will & inspiration helped us a lot in completing this project work.



Miss. Mrunali Tanaji Nikam

B.Sc (Physics)



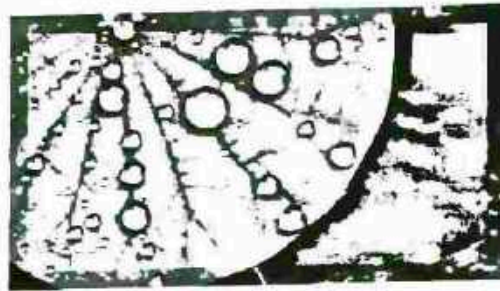
INDEX

Chapter No.	Chapter Name	Page no
1	Introduction to Natural Superhydrophobic Surfaces	01 to 12
2	Methodology and Characterization Techniques	13 to 26
3	Experimental research work	27 to 40
4	Conclusion	41 to 42



Chapter 1

Introduction to Natural Superhydrophobic Surfaces.



CHAPTER 1
INTRODUCTION

1.1	Introduction	
1.2	Natural Superhydrophobic Surfaces	
	1.2.1	Lotus Leaf
	1.2.2	Cabbage
	1.2.3	Cicada Wings
	1.2.4	Butterfly Wings
1.3	Wettability and their types	
1.4	Oil-water separation	
1.5	References	



CHAPTER 1

Introduction to Natural Super hydrophobic Surfaces.

1.1 Introduction

Superhydrophobicity was first observed in the nature on lotus leaf and in some other plants in which their leaves would not get wet. The main reason of this phenomenon was the unique surface structure of the lotus leaf and also presence of a low surface energy material on the surface of the leaf. In order to achieve superhydrophobic surface or coating, the surface must possess hierarchical micro- and nano-roughness and low surface energy at the same time. Hierarchical micro- and nanoscale roughness will trap air on the surface that will cause increase in water contact angle, and low surface energy will decrease the tendency of water to have bonding with the surface. So, almost all the methods to achieve super hydrophobicity consist of two steps: first to make a hierarchical surface roughness and then surface modification by a low surface energy solution of some materials like fatty acids, fluoroalkyl silanes, etc.[1]

Super hydrophobic surfaces have evoked great interest in researchers for both purely academic pursuits and industrial applications. Many review articles covering different aspects of superhydrophobicity have been published (Bhushan and Jung, 2011, Ma and Hill, 2006, Nakajima et al., 2001, Quere, 2005, Roach et al., 2008, Xue et al., 2010). Superhydrophobic surfaces (SHS) exhibit extremely high water repellency, where water drops bead up on the surface, rolling with a slight applied force, and bouncing if dropped on the surface from a height.

It is well known that the degree to which a solid repels a liquid depends upon two factors: surface energy and surface morphology. When surface energy is lowered, hydrophobicity is enhanced. Chemical compositions determine the surface free energy and thus have a great influence on wettability (Woodward et al., 2000). However, certain limitations are encountered and superhydrophobic surfaces cannot be obtained only by lowering the surface energy. For example, the $-CF_3$ - terminated surface was reported to possess the lowest free energy and the best hydrophobicity, but the maximum contact angle on flat surfaces could only reach 120° (Nishino et al., 1999).[2].

In superhydrophobic surface, the surface morphology plays a crucial role effecting wettability. Roughening a surface can not only enhance its hydrophobicity due to the



increase in the solid–liquid interface (Wenzel, 1936, Wenzel, 1949) but also when air can be trapped on a rough surface between the surface and the liquid droplet. Since air is an absolutely hydrophobic material with a contact angle of 180° , this air trapping will amplify surface hydrophobicity (Ogihara et al., 2013, Sun et al., 2005). Hierarchical micro- and nanostructuring of the surface is thus responsible for superhydrophobicity. [3].

In case of the mosquito eyes, its surface morphology depicts close packed hemispheres at micro scale and hexagonally non-close packed nipples at nanoscale. Superhydrophobicity and antifogging properties are provided by nipples and hemispheres, which prevent moisture from accumulating and forming spherical drops on the mosquito's eye surface, allowing the mosquito to see clearly [4]. A water strider moves elegantly over the water's surface due to its non-wetting legs which are decorated by needle-shaped microsetae and that are inclined at a 20° angle to the surface [5,6]. A gecko feet reveals metastable superhydrophobic property where the water droplets endure adhering on the foot even if rotated upside down [7].

Comprehensive surface analysis of the natural superhydrophobic surfaces has confirmed that the surface micro/nanostructure along with low surface energy chemical compounds is an essential requirement for high water repellency. According to the Wenzel [8] to the Cassie-Baxter [9] model, the hydrophobicity can be upgraded by increasing and optimizing the magnitude surface roughness value. In Wenzel-type rough surface, water droplet penetrates the rough structure, however maintains high contact angle (CA) by locking the water drop over it. Whereas, in Cassie and Baxter type rough surface, air pockets are imprisoned into the rough surface, which reduces that attraction of the water drop on it. On such surface, water droplets do not infiltrate the rough structure due to the air-solid interface and hence the droplets quickly displaced from the surface by small inclination. Natural superhydrophobic surfaces have grabbed the attention of researchers to develop artificial superhydrophobic surfaces by mimicking their micro/nanostructure using various physical and chemical methods for self-cleaning [10], anti-icing [11], anti-fogging [12], anti-wetting [13], anti-fouling [14], anti-bacterial [15], anti-drag [16], anti-corrosion [17], oil-water separation [18] and many other [19] applications.

1.2 Natural Superhydrophobic Surfaces

There are several examples of natural superhydrophobic surfaces, e.g., plants and insects. The most remarkable natural superhydrophobic surface is the lotus leaf. The high hydrophobic degree by lotus leaf inspired researchers to do initial research on the hydrophobic phenomenon.

The natural world is full of hydrophobic and hydrophilic surfaces, the basics of the phenomenon have been known by scientists for at least two centuries. For example, the



lotus leaf is a well-known example of a hydrophobic material, protecting the water-dwelling plant from becoming waterlogged.

1.2.1 Lotus Leaf

Since the introduction of the 'Lotus concept' in 1992, the lotus leaf became the archetype for superhydrophobicity and self-cleaning properties of plant surfaces and a model for technical analogues. Lotus (*Nelumbo nucifera*) is a semi-aquatic plant and develops peltate leaves up to 30 cm in diameter with remarkable water repellency. As an adaptation to the aquatic environment – some of the leaves float occasionally on the water surface – the stomata are located in the upper epidermis. The lower epidermis consists of convex cells covered with wax tubules and contains only few stomata. The upper epidermis features the distinctive hierarchical structure consisting of papillae with a dense coating of agglomerated wax tubules, which is the basis for the famous superhydrophobicity [21] (Figure 1).

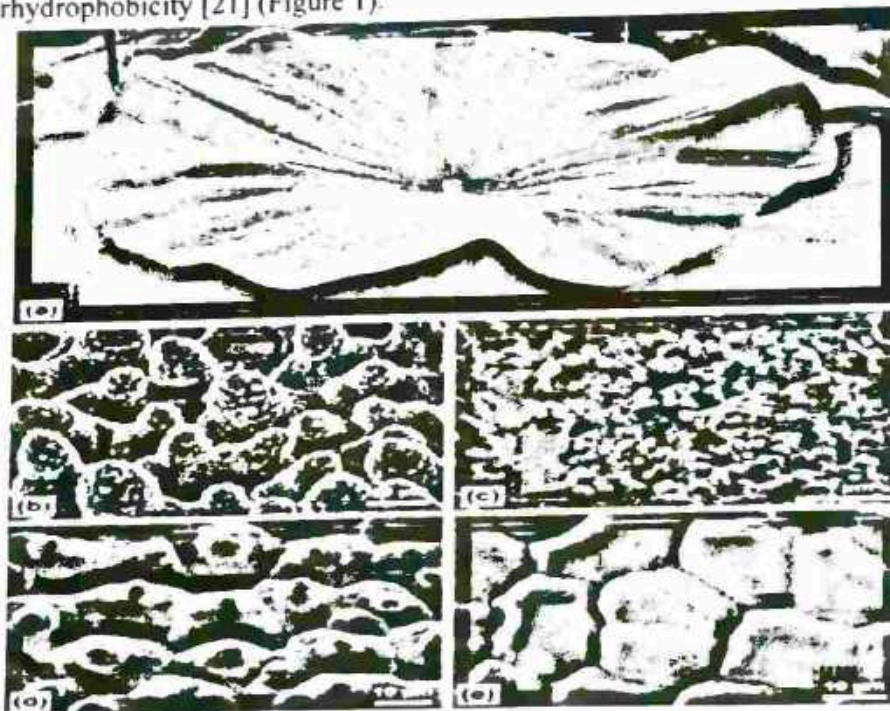
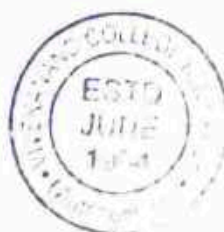


Figure 1: (a) Lotus leaves, which exhibit extraordinary water repellency on their upper side. (b) Scanning electron microscopy (SEM) image of the upper leaf side prepared by 'glycerol substitution' shows the hierarchical surface structure consisting of papillae, wax clusters and wax tubules. (c) Wax tubules on the upper leaf side. (d) Upper



leaf side after critical-point (CP) drying. The wax tubules are dissolved, thus the stomata are more visible. Tilt angle 15° . (e) Leaf underside (CP dried) shows convex cells without stomata.

However, a hierarchical surface structure which induces strong water repellency and contact angles above 150° is not a special feature of lotus leaves. It has been known for a long time that plant surfaces covered with epicuticular wax crystals are water repellent, and that this feature is enhanced when the epidermis has additional structures such as papillae or hairs, Neinhuis and Barthlott (1997) presented an overview of more than 200 species with contact angles $>150^\circ$ and their surface morphologies. Many studies, in which the properties of lotus leaves were compared with those of other superhydrophobic plants, have shown the superiority of the upper side of the lotus leaf. A standard tool for the determination of wettability or water repellency is the measurement of the static contact angle by the 'sessile drop' method. Neinhuis and Barthlott (1997) for example, measured contact angles on the lotus leaf of 162° , which are among the highest of the compared species, but many other (43%) of the tested superhydrophobic plants also showed contact angles between 160 and 163° . Even some species with flat epidermis cells but with a dense layer of epicuticular wax crystals, such as *Brassica oleracea* or some *Eucalyptus* species, can exhibit contact angles $>160^\circ$. Thus, the contact angle alone is not suitable for a differentiated comparison of superhydrophobic samples.[22]. Other values such as contact angle hysteresis or roll-off (tilting) angle show more clearly the differences between the species. Mockenhaupt et al. (2008) compared the tilting angles and the stability of the superhydrophobicity of various plants under moisture condensation conditions. Only the lotus leaves showed no significant loss of water repellency when water vapour condensed on the surface of the cooled samples at 5°C . Wagner et al. (2003)[23] . examined the morphology of the epidermal structures and the wettability with liquids of varying surface tension such as methanol–water mixtures. They reported the lowest wettability by these liquids for the lotus leaves in comparison to other species. They also described the unique shape of the papillae and a very high papillae density (number per area). Chemical analyses and crystal structure analysis by X-ray diffraction showed unique properties of the epicuticular wax of the lotus. The high content of nonacosanediols leads to a high melting point as well as a strongly disturbed crystal structure which is the basis for the formation of tubules. The visualization of the contact zone between leaves and droplets with cryo-scanning electron microscopy demonstrated the extremely reduced contact area for lotus . Zhang et al. (2008) [24] made detailed measurements of the water repellency of the papillose lotus leaf surface in comparison with the non-papillose leaf margin. The importance of the nanoscopic wax crystals for the water repellency was demonstrated by Cheng et al. (2006)[25] . They reported a strong decrease of the contact angle after melting of the waxes. A limited air retaining capability of submersed lotus leaves was reported by Zhang et al. (2009) [26] after the leaves were



held at a depth of 50 cm for 2 h. Bhushan et al. (2010) [27] used the surface structures of the lotus leaf as model for the development of artificial biomimetic superhydrophobic structures.

It became obvious that the outstanding and stable superhydrophobicity of the lotus leaf relies on the combination of optimized features such as the surface topography, robustness and the unique properties of the epicuticular wax. The aim of this article is to integrate the relevant features of the lotus leaf, and to compare them with superhydrophobic leaves of other plant species in order to illustrate their significance.[28].

1.2.2 Cabbage

When we wash plants in the cabbage family (which includes Brussel sprouts and broccoli), we see that water easily bounces off the leaves. This is a clear indication that they are superhydrophobic. The superhydrophobicity is caused by wax towers on the surface of the leaves. We can see this in the Scanning Electron Microscope (SEM) picture on the right below. The structure is quite different to that of the lotus, which looks more like a collection of hillocks, even though they have bumpy waxy surfaces.



Figure 2. Water drop in a cauliflower leaf. Image courtesy of Lynn Greyling, CC0 Public Domain license



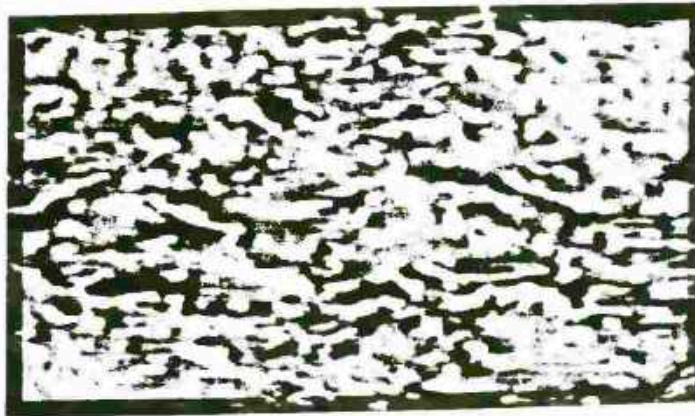


Figure 3. SEM image of a cabbage leaf

Hydrophobicity can present a problem for farmers wanting to spray plants that are diseased or have been attacked by insects because sprays can bounce off them just as water does. Fortunately, the addition of a little surfactant to the spray prevents this. Surfactant is usually present in commercial spray formulations [29].

1.2.3 Cicada Wings

The superhydrophobicity of insect wings is an advantage to reduce the dust/particle contamination and to enhance their flight capability. The group of Barthlott studied the surface structures and wettability of 97 insect wings [30]. They found different families with highly hydrophobic wings including mayflies, dragonflies, stoneflies, lacewings, scorpionflies, alderflies, caddisflies, butterflies, moths and flies, as reported by Watson and coworkers for termite wings. Various morphologies were reported, such as cloth-like microstructures, hairs or scales. They also found that the transparent wings of cicada are due to a single level of roughness consisting of regular patterns of nanopillars, confirming works reported by Yoshida et al. on the transparency of hawkmoth wings (*Cephonodes hylas*). Indeed, it is possible to have both superhydrophobic and transparent properties by playing on the size of the nanostructures, as the decrease in the transparency is due to the light scattering inside the surface roughness. Sun et al. also analyzed the wings of 15 species of cicada (Fig. 4). They observed differences in the homogeneity of the nanodomains as well as differences in their diameter (\emptyset), height (h) and spacing (s). The highest water-repellent properties were obtained for *Terpnosia jinpingensis* for which $\emptyset = 141$ nm, $h = 391$ nm and $s = 46$ nm. However, a water droplet deposited on these surfaces remained pinned on it, indicating high adhesion (impregnating Cassie–Baxter state). By contrast, Watson et al. also reported that the wings of another species of cicada (*Psaltoda claripennis*) with $h \approx 200$ nm and $s \approx 200$ nm were superhydrophobic but with ultra-low adhesion for particles. A natural extension of investigations of air-borne particle adhesion with insect



wings as suggested by the studies of Watson et al. was the examination of solid contacts of insect cuticle under aqueous conditions. Such studies include those by Ivanova et al. demonstrating that cicada wings possess the ability to selectively kill Gram-negative bacteria, while Gram-positive bacteria were not killed. Hence, nanostructured surfaces can open new strategies to develop bactericidal surfaces without biocides.

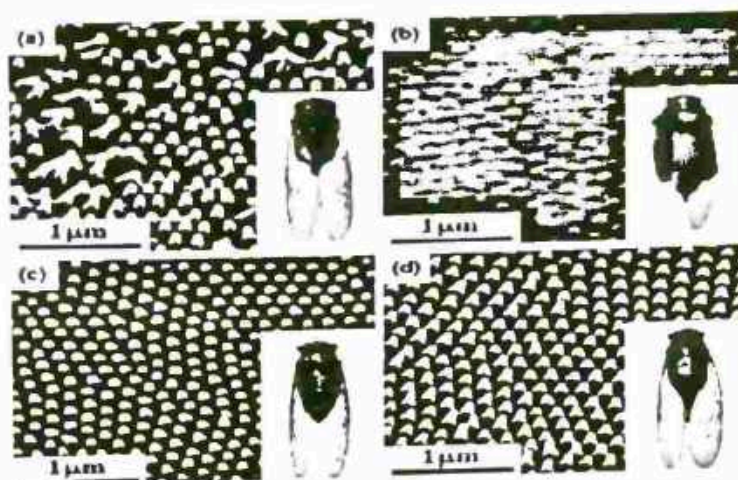


Figure 4. Images of the nanostructures present of different species of cicada.

The chemistry of superhydrophobic insect wings has also been investigated by several-9 research groups. For example, Ivanova et al. showed that dragon fly wings are coated by waxes, as observed in superhydrophobic leaves .

As observed in cicada wings, the presence of highly ordered nanostructures can also lead in certain cases, to colored as well as iridized materials, without the presence of dyes, if the nanostructures can diffract the light and induce interference effects . The color of the material is directly dependent on the size of the structures . The group of Goodwyn studied the structures of different butterflies having hydrophobic or superhydrophobic properties and different colors . While the scales of the transparent butterfly wings of the genus *Parnassius glacialis* (Papilionidae) displayed no clear pattern the white translucent regions of *Parantica sita* (Nymphalidae) were highly ordered and organized in lines forming periodic and parallel porous microstructures. Prum et al. also demonstrated that the color of twelve butterflies (Lepidopteran species) is due to appropriate nanostructures in their scales producing visible colors, such as blue, green, or violet. Moreover, at the microscale, the scales of butterflies, such as *Morpho aega*, overlap in only one direction. As a consequence, the wings of these species are superhydrophobic but with directional adhesion, also called anisotropy . When a water droplet is deposited on the wing, it can roll off the surface only if the wing is inclined in one direction .



1.2.4 Butterfly wings

The wings of the butterfly shows the anisotropic superhydrophobic property. The structural color, as well as its chemical sensing and fluorescence emission capabilities, are all visible on butterfly wing surface. Moreover, it displays self-cleaning property and high hydrophobicity. Fang et al. have investigated the wing surface of species 29 of butterfly. The surface of wing's is composed of micro- to submicro-class vertical gibbosities and they have arranged in scale pattern like an overlapping tiles, therefore the wing surface exhibited a CA between 136° – 156° . A droplet moved along the radially outer direction, on the contrary, pinned tightly in reverse over wing surface. A SEM image of butterfly wing reveals that wing is composed of quadratic form having $150\ \mu\text{m}$ length and $70\ \mu\text{m}$ width, which provides a regular hierarchy in the radially outer direction by overlapping each other.

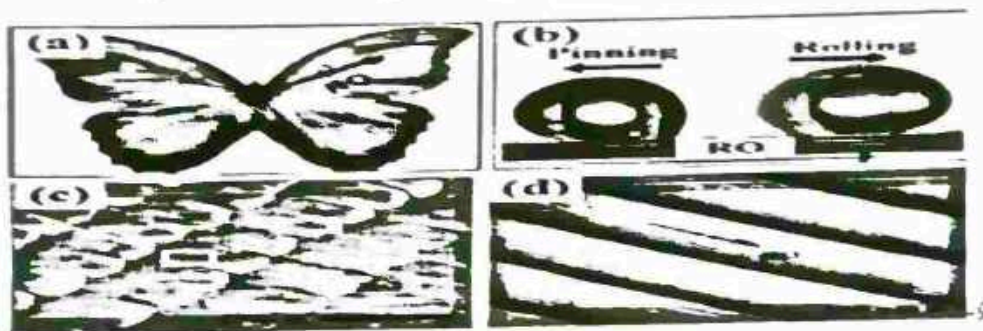
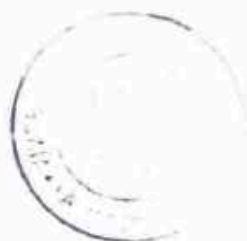


Figure. 5 (a) Photograph of butterfly *M. aega*, the arrow denotes the radially outer (RO) direction. (b) photograph of water drop pinning and rolling on the butterfly wing surface, SEM images of the (c) regular arrangement of overlying micro-scales on the wings and (d) fine lamella-stacking nano-stripes on the scales.

A magnified SEM image reveals single ridging stripes of width of $184.3 \pm 9.1\ \text{nm}$ on the surface of each scale (Fig. 5 (d)). Interestingly, the back side of a butterfly's (*Papilio ulysses*) wing displayed long-term superhydrophobic property under water than the front side. By soaking both sides of the butterfly wing in deionized water for 60 h and changes in the CA were measured. The existence of a large amount of hair (length about $200\text{--}600\ \mu\text{m}$) on the back side of the wing of butterfly could resist the water moving inside the wing. Wanasekara et al. have examined the influence of nanostructure on the wettability and factor of restitution of four different butterflies (*Greta Oto*, *Phoebis Philea*, *Antheraea Polyphemus*, *Actias Luna*) wing surfaces. Due to the combination of micro scales as well as hair like microtrichia, the *Actias Luna* showed high roughness factor along with high static and dynamic CA. The distinct microstructure of the butterfly wing surface resulted in a different coefficient of restitution. Mei et al. have reported the superhydrophobicity of butterfly wings can exist in low-temperature environment as well as at low relative humidity.



1.3 Wettability and Their Types

Wetting is the ability of a liquid to maintain contact with a solid surface, resulting from intermolecular interactions when the two are brought together. This happens in presence of a gaseous phase or another liquid phase not miscible with the first one. The degree of wetting (wettability) is determined by a force balance between adhesive and cohesive forces.

Wetting is important in the bonding or adherence of two materials.[1] Wetting and the surface forces that control wetting are also responsible for other related effects, including capillary effects.

There are two types of wetting: non-reactive wetting and reactive wetting.

Wetting deals with three phases of matter: gas, liquid, and solid. It is now a center of attention in nanotechnology and nanoscience studies due to the advent of many nanomaterials in the past two decades (e.g. graphene, carbon nanotube, boron nitride nanomesh).

Wettability can be measured through contact angle. Typically, 90° contact angle is considered as a threshold value. When the contact angle is above 90° , the wettability is bad, when it is below 90° the wettability is good. Wettability of a solid surface is commonly measured with an optical tensiometer by utilizing the sessile drop method.

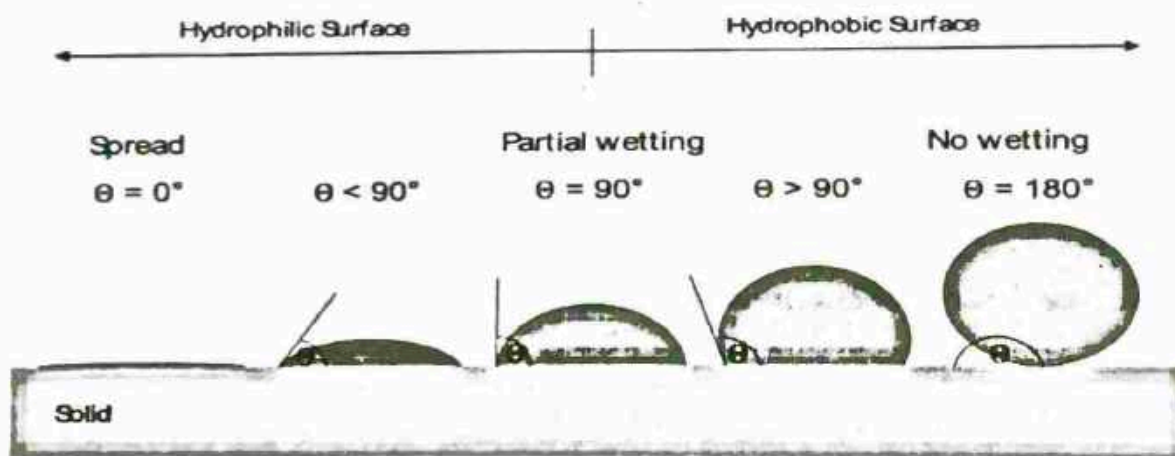


Fig 6 The wettability in terms of contact angle

The wetting behavior of a solid surface is not only determined by its chemical properties but also by its surface roughness. This relationship between surface roughness and wettability has been extensively studied by scientists, including Cassie-Baxter and Wenzel. They observed that on rough solid surfaces, two distinct states can be observed. Surface roughness can be achieved by etching the solid surface, and when a water drop is placed on the surface, it either fills the cavities on the rough surface or lies above them. In the Cassie-Baxter state, the water drop does not wet the entire surface and instead lies above the cavities, resulting in a larger



contact angle. In contrast, in the Wenzel state, the water drop wets the entire surface, including the cavities, resulting in a decrease in contact angle. Wenzel also proposed that as the surface roughness increases, the hydrophobicity of hydrophobic surfaces and the hydrophilicity of hydrophilic surfaces increases. In summary, the wetting behavior of a solid surface is determined by a combination of its chemical properties and surface roughness. Understanding the relationship between surface roughness and wetting behavior is crucial in designing surfaces with specific wettability properties for various applications. The following figure will elaborate both the Cassie-Baxter and Wenzel states.

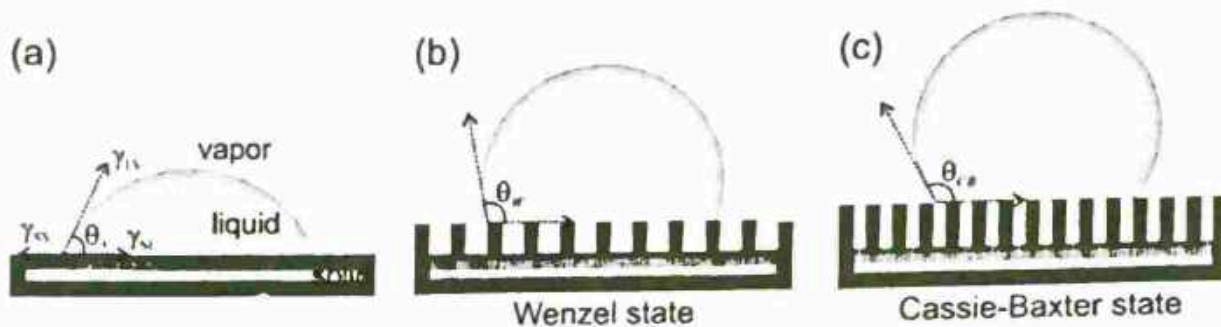


Fig 7: The Cassie-Baxter State And The Wenzel State

1.4 Oil Water Separation

The process of oil-water separation involves the creation of a surface that is able to selectively interact with oil and water. This is achieved by designing a surface with specific surface properties that enable the separation of the two liquids. A superhydrophobic surface is one such surface that has been found to be highly effective in separating oil and water. Superhydrophobic surfaces are characterized by their high water repellency and low surface energy. This means that water droplets do not wet the surface and instead form spherical droplets that easily roll off the surface. These surfaces are created by modifying the surface properties of a material, such as its texture or chemical composition, to produce a surface that is highly water repellent. To separate oil and water using a superhydrophobic surface, the surface is designed to have pores or channels that are smaller than the size of the oil droplets. This allows the oil droplets to pass through the pores while the water droplets are blocked and cannot pass through. The oil droplets are then collected and separated from the water. There are several techniques that can be used to create superhydrophobic surfaces for oil-water separation. One common technique is to create a surface with micro or nanoscale structures that trap air pockets, which prevent water from wetting the surface. Another technique is to modify the chemical composition of the surface to make it highly hydrophobic. In addition to their use in oil-water separation, superhydrophobic surfaces have many other potential applications. They can be used



to create self-cleaning surfaces, anti-fogging surfaces, and anti-icing surfaces. They can also be used in biomedical applications to create anti-bacterial surfaces and in environmental applications to separate pollutants from water. The use of superhydrophobic surfaces for oil-water separation is a promising technology that has the potential to significantly reduce the environmental impact of oil spills and improve the efficiency of oil recovery operations. By creating surfaces that selectively interact with oil and water, we can develop more effective and sustainable methods for oil-water separation.

1.6 References :

- [1] Liu, Kesong, Xi Yao, and Lei Jiang. "Recent developments in bio-inspired special wettability." *Chemical Society Reviews*, 3240-3255, 2010.
- [2] L. Feng, S. Li, Y. Li, H. Li, L. Zhang, J. Zhai, Y. Song, B. Liu, L. Jiang and D. Zhu, "Super-hydrophobic surfaces: from natural to artificial", *Advanced Materials*, 14 (2002) 1857.
- [3] Thierry Darmanin, Frédéric Guittard, " Superhydrophobic and superoleophobic properties in nature " *Materials Today*18(5), 2015, 273-285.
- [4] Y. Fang, G. Sun, T. Wang, Q. Cong, and L. Ren, , " Hydrophobicity mechanism of non-smooth pattern on surface of butterfly wing,"*Chinese Science Bulletin*, 52 (2007) 711.
- [5] W. Barthlott, M. Mail, B. Bhushan and K. Koch, "Plant surfaces: structures and functions for biomimetic innovations ", *Nano-Micro Letters*, 9 (2017) 23.
- [6] C. Neinhuis and W. Barthlott, "Characterization and distribution of water-repellent, self-cleaning plant surfaces, *Annals of Botany*", 79 (1997) 667.
- [7] X. Gao, X. Yan, X. Yao, L. Xu, K. Zhang, J. Zhang, B. Yang, and L. Jiang, The dry-style antifogging properties of mosquito compound eyes and artificial analogues prepared by soft lithography, *Advanced Materials*, 19 (2007) 2213.
- [8] X. Gao, and L. Jiang, Water-repellent legs of water striders, *Nature*, 432 (2004) 36.



Chapter 2

Methodology and Characterization Techniques



CHAPTER 2
METHODOLOGY AND CHARACTERIZATION

2.1		Deposition Techniques
	2.1.1	Dip coating method
	2.1.2	Spin coating method
	2.1.3	Spray coating method
	2.1.4	Electrodeposition technique
	2.1.5	Sol gel process
2.2		Superhydrophobic surfaces and their application
2.3		Characterization Techniques
	2.3.1	Scanning electron microscope
	2.3.2	Transmission electron microscope
	2.3.3	Atomic force microscopy
	2.3.4	Wettability
2.4		References



Chapter 2

Methodology and Characterization Techniques.

2.1 Deposition Techniques.

2.1.1 Dip Coating Method

Dip coating is a simple, low-cost, reliable and reproducible method which involves the deposition of a wet liquid film by immersion of the substrate into a solution containing hydrolysable metal compounds (or readily formed particles) and its withdrawal at constant speed into an atmosphere containing water vapor.

Dip coating has been extensively utilized for research purposes owing to it being a convenient and facile approach. The quality of the coatings produced by this way, nonetheless, is inconsistent, and therefore, it is an inappropriate approach for industrial processes. The critical parameters that can affect the coatings produced by dip coating are shown in Fig. 1. Generally, dip coating consists of a five-step process, including:

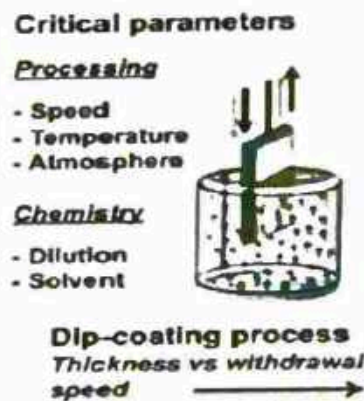


Figure 1. The critical parameters affecting the coatings produced by the dip-coating method.

1. Immersion: At a constant speed, the substrate is dipped into the coating solution. Based on the kind of the substrate, a pretreatment process would be carried out before this step.

2. Startup: The substrate remains in the solution for a designated time, and then it starts to be pulled out.

3. Deposition: While the substrate is being pulled out, the thin film coating starts to be deposited on it. The thickness of the coating is directly dependent on the speed by which the substrate is being pulled out. The slower pull, the thinner the coating layer.

4. Drainage: In this step, excess liquid is drained from the substrate surface.



5. Evaporation: Solvent starts to evaporate from the surface of the substrate to form a thin film. If the solvent is volatile, this step might happen in step 3.

Because no sophisticated equipment is required for this method, it is much more convenient and facile than the other approaches. The coating layer produced, nevertheless, may not be of good quality, due to the simplicity of the method. Relating to graphene-based composite coatings, the thickness distribution may be an issue. For pristine graphene-based material coatings, the coating layer produced might not be sufficiently dense to show superior properties, and as well, the applied substrate cannot be vastly large and complicated. However, dip coating can still be utilized at large scale to produce products fulfilling low standard requirements at a competitive price, although it is more appropriate for use in the lab. Since graphene-based composite coatings possess much higher viscosity in contrast with pristine graphene-based coatings, resulting in not only a better interfacial adhesion toward a substrate but also a more uniform coating layer, this method is more appropriate to produce this kind of coating. A subsequent treatment process may be required to form a solid coating layer.

2.1.2 Spin Coating Method

Spin coating is the simplest method for fabricating a film on a substrate. Thin-resist layers for photolithography are coated with this technique. The spin-coating process starts with the dilution of the material to be deposited in a solvent. The solution is subsequently dispensed on the substrate surface. The wafer is then spun at a high speed. The thickness of the film is determined by the spinning speed, surface tension, and viscosity of the solution. The solvent is removed partly during the spinning process due to evaporation and partly by subsequent baking at elevated temperatures. Spin coating results in a relatively planar surface. This technique is often used for planarization purposes. Spin coating can be used for the deposition of sol-gels. In this process, solid particles of a polymer compound dissolved in a solvent are spin-coated on the substrate surface. The process forms a gelatinous network on the substrate surface. Subsequent removal of the solvent solidifies the gel, resulting in a solid film. This technique can be used for the deposition of various ceramics, such as lead zirconate titanate (PZT). Besides spin coating, dry lamination, dip coating, spray coating, and electrodeposition can be used for transferring a resist layer to the substrate surface.





Figure 2 : Spin coating process

2.1.3 Spray Coating Method

Spray coaters can be classified into three major groups according to the spray method: Air spray systems, ultrasonic spray systems, and electrostatic spray systems.

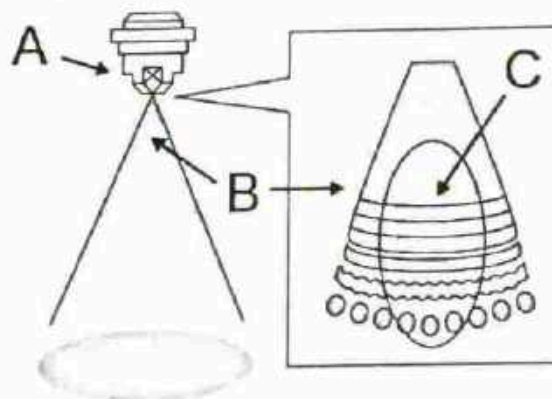


Figure 3: Air Spray System

A. Nozzle B. Coating fluid C. Atomization through collision with air.

Air spray systems use compressed air to change the coating fluid into a fine mist that is sprayed onto the target. A typical example is an air spray gun, which uses a similar mechanism. Compressed air applies high pressure to the coating fluid discharged from the nozzle and the fluid then collides at a high speed with the remaining air. The coating fluid is split up and slowed down at that moment due to air resistance, and then changes into a mist before reaching the target. Air spray systems are generally said to disperse too much coating fluid, causing a relatively excessive loss of material. The equipment, however, has been designed to be



sophisticated and diverse. For example, some systems use a nozzle that can change the coating fluid into a fine mist that allows uniform coating of uneven surfaces, while others can maintain high-speed spraying that enables stable coating. Other systems are capable of advanced movement control and automation of the stage and nozzle. A variety of products are available according to the target area, required efficiency, and coating purpose.

2.2.4 Electrodeposition Techniques.

In this, SHC coating is the result of chemical reactions of electrolytic solution which is triggered by the application of current .

Schematic representation of electrochemical deposition is shown in fig. 4. Anodic oxidation, deposition using galvanic cell, polymerization, and electrochemical anodization, etc, are some of the production techniques that make electrochemical deposition a wide method for the fabrication of SHC .Yan Liu et. al. successfully fabricated SHC on a copper plate via electrochemical deposition. They had taken 2 copper for the anode and cathode. The electrolytic medium used for this process was a mixture of cerium chloride, myseric acid, and ethanol. Zengguo Bai and Bin Zhang have prepared a novel reduced graphene oxide rGO/Ni composite coating on stainless steel through electrodeposition. They deposited a thin layer of Ni on the substrate before the application of the rGO/Ni composite layer. The electrolyte they used as the medium was prepared by adding $NiCl_2 \cdot 6H_2O$, orthoboric acid, potassium chloride, sodium dodecylbenzene sulfonate, and rGO. The superhydrophobic coatings were generated by the deposition of Ni on the stainless-steel substrate followed by the deposition of rGO /Ni composite mix.

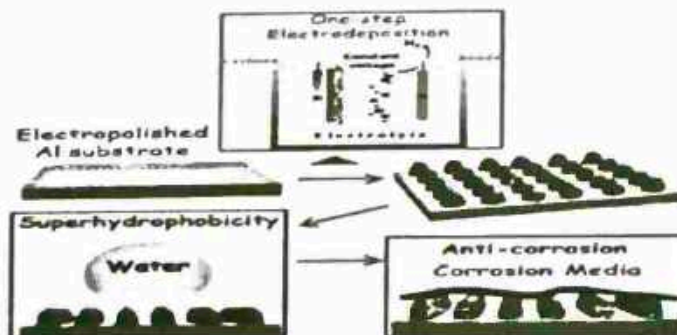
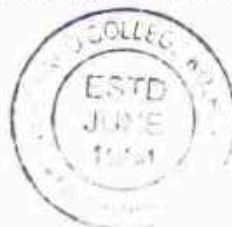


Figure :4: Schematic representation of electrochemical deposition coating on Al substrate .



2.1.5 Sol-gel process

The sol-gel process is the most preferred method for developing good quality coatings. The inorganic silica and organically modified silanes comprise a hybrid sol-gel that forms a 3D network to impart superhydrophobic character to the coated surface .

Spray coating, spin coating, and dip coating are the 3 techniques that can be used to deposit the sol-gel on various substrates . Fig. 5 shows the schematic representation of the Sol-gel coating technique. S. Liu et al reported the synthesis of transparent SHC via sol-gel processing of long-chain Fluoroalkylsilane. The coating mix was prepared by adding ethanol (solvent), ammonia (catalyst), and water. The final super repellent surface was achieved by the immersion of glass in the prepared solution for different deposition times.

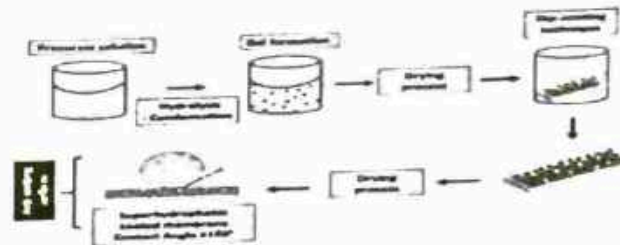


Figure 5: Schematic representation of sol-gel coating technique

2.2 Super hydrophobic surfaces and their Application.

Superhydrophobic surfaces are characterized by their extremely high water repellent property. When a water drop is placed on such surfaces, it attains a circular shape, and the contact between the water drop and the superhydrophobic surface is minimized, resulting in a higher contact angle. Moreover, if the surface is tilted, the water drop on the surface rolls or slides off very easily. The sliding angle for superhydrophobic surfaces is typically less than 10°. The unique property of superhydrophobic surfaces in not allowing water drops to stay on the surface has led to a wide range of applications. Some of these applications include self-cleaning surfaces, anti-icing surfaces, anti-corrosion coatings, and oil-water separation devices. Superhydrophobic surfaces are also used in microfluidic devices for droplet manipulation and in the development of water-repellent fabrics and coatings for various outdoor applications.

1. Self-cleaning

Superhydrophobic surfaces are capable of self-cleaning. When water is sprinkled on a dusty superhydrophobic surface, the water drops form circular shapes and roll off from the surface, collecting dust particles along the way. This makes the surface clean. This property of the superhydrophobic surfaces is known as the self-cleaning property. It can be applied to surfaces such as windows, outer walls of buildings, and many more.

2. Corrosion resistant



Superhydrophobic surfaces have water-repellent properties, preventing water from staying on the surface. This characteristic helps decrease corrosion and increase the corrosion resistance of the surface. Corrosion occurs when metals react with oxygen and corrode.

3. Anti-fogging surfaces

Superhydrophobic surfaces prevent water drops from remaining on the surface. This characteristic makes them anti-fogging surfaces. Water droplets that form on mirrors, windows, etc. due to fog will not remain on superhydrophobic surfaces and roll off instead.

4. Anti-bacterial surfaces

In the medical field, cleanliness is of great importance. All surgical instruments should be sterilized and free from bacteria. Superhydrophobic surfaces are used for this purpose because they prevent bacteria from sticking to the surface. When bacteria cannot stick to a surface, it cannot grow and spread.

5. Anti-icing surfaces

In snowy areas, snow accumulates on various surfaces such as highways, industries, aircraft, and vehicles. Physical and chemical methods used to remove ice may cause damage and consume much energy. Superhydrophobic surfaces help reduce the chances of damage and conserve energy.

2.3 Characterization Techniques

Characterization and analytical techniques are methods used to identify, isolate or quantify chemicals or materials, or to characterize their physical properties.

2.3.1 Scanning Electron Microscope[SEM]

In general, a scanning electron microscope (SEM) can make images of solid samples and can determine the elemental composition of said samples. The low end of the magnification range for an SEM is typically on the order of 20X to 50X. The maximum magnification is generally determined by the size of the electron beam and can be as high as one million (10^6). These magnification levels generally correspond to measuring features from the mm scale down to nm size. The best resolution of a high end SEM is on the order of 0.5 nm. The most common type of SEM data is the secondary electron image. The SE image is a map of secondary electron emission as a function of spatial position. SE images generally display the topography of the sample. The number of secondary electrons emitted from a surface generally depends on the angle of incidence between the surface and the beam. Since the electron beam is perpendicular to the sample over the analysis area, the number of secondary electrons emitted from the sample is



generally a function of the topography of the sample. Backscattered electrons (BSE) are the second most common imaging data collected with an SEM. This data is a map of backscattered electron emission as a function of spatial position. The number of BSEs that are emitted is a function of the atomic number of the sample. As the atomic number increases, so does the number of BSEs emitted. This means that images made with BSEs will generally show the composition of the sample. While it is not generally possible to observe a BSE image and know what materials are present, with some a priori knowledge of the sample's composition, it is usually possible to make a good guess about the material distribution from a high quality BSE image. It is possible to combine BSE images with EDS to determine both the material composition and distribution in the sample. Since images are in the form of the electron emission from a sample vs. spatial position, it is not possible to determine the roughness of a sample from a plane view image of the sample as the electron emission from the sample may not depend on the height. Even if the electron emission does depend on the height, as in a secondary electron image, measuring a height from the electron emission is not generally possible. Roughness can only be determined from a cross-section of the sample. In addition to collecting imaging data to show the morphology of a sample, SEMs also generate and can collect X-rays that are characteristic of the elements in the sample. This is usually done with an energy dispersive X-ray spectrometer or EDS system. EDS X-ray data can be used to determine the elements in the sample. If the X-ray data is mapped as a function of spatial position, an X-ray map showing the distribution of the elements in the sample can be created. The detection limit for EDS is generally on the order of 0.5% by weight within the X-ray generation volume.

2.3.2 Transmission Electron Microscopy (TEM)

Transmission Electron Microscopy (TEM) provides powerful techniques for understanding various information of materials at very high spatial resolution, including morphology, size distribution, crystal structure, strain, defects, chemical information down to atomic level and so on. All the information that TEM can give to us are from electron-sample interaction. The transmitted electrons that have passed through the thin sample are detected to form images, which is the reason to call it "transmission" electron microscopy. In order to allow electrons to transmit through the sample, TEM sample must be very thin (typically, sample thickness is less than 200 nm, depending on the composition of sample and the expected information from TEM characterization). There are many techniques in transmission electron microscopy, which can give you different information about your samples. Some techniques are listed below:

1. Selected-area electron diffraction (SAED). One of the two basic operations of TEM imaging system, i.e. diffraction mode and imaging mode. For SAED, a selected area aperture is inserted into the image plane to virtually select an area from the sample to form diffraction pattern. SAED can be used to identify crystal structures, nanowire growth direction, tell crystallinity and set up conditions for dark field imaging.



2. Bright field (BF) TEM. BF images are formed by the direct-beam (transmitted beam) electrons, only very few scattered electrons can pass the aperture to contribute to the imaging.

3. Dark field (DF) TEM. An objective aperture is inserted into the back focal plane (where diffraction pattern is formed in the reciprocal space) to select scattered electrons. Typically, a specific diffracted beam (single crystalline) or a portion of a diffraction rings (polycrystalline) can be used for DF imaging. DF images can usually give information on nanocrystal size distribution and crystalline defects, such as stacking faults, twinning, and dislocations.

4. High-resolution TEM (HRTEM). The imaging mechanism of HRTEM is phase contrast, which uses the interference of the transmitted beam and diffracted beams to form images at atomic level. HRTEM is useful for the imaging of atom arrangements in projection. This technique normally requires very thin samples (less than 15 nm in thickness, as thin as possible). The interpretation of HRTEM images is always challenging.

5. High angle annular dark field (HAADF) – STEM imaging. HAADF-STEM imaging collects incoherently scattered electrons at high angles to form images, which gives contrast dependent on atomic number and specimen thickness. It is also called Z contrast.

6. Energy-dispersive X-ray spectroscopy (EDS). EDS can provide compositional or chemical characterization. Our Titan with ChemiSTEM technology can collect X-ray much more efficiently. The four windowless silicon drift detectors (SDDs) can provide a solid angle of 0.7sr. X-FEG can provide 5 times more electrons compared to a conventional Schottky FEG source. Overall, it can collect up to 10 times X-ray compared to conventional single-SDD.

7. Electron energy loss spectroscopy (EELS). When electrons pass through the sample, some electrons are getting inelastically scattered and results in both energy loss and a change in momentum. These energy losses are characteristic for the elements in the sample. A typical EEL spectrum contains zero loss peak, low loss and core loss regions. Zero loss peak is formed by elastically scattered electrons with zero energy loss and electrons that do not interact with the sample, from which we can get the sample thickness (also need the sum of inelastically scattered electrons). Low loss region is formed by electrons with low energy losses, which can give information on sample optical properties. Core loss region is formed by electrons with energy losses by ionization of core shells, which can provide information on elemental composition and concentration, as well as bonding/valence state. Very thin samples (less than 50 nm in thickness) are required for EELS analysis.

8. Energy-filtered TEM (EFTEM). Only electrons with particular energy losses (“energy windows”) are chosen by energy slit to form images. Since the energy losses are characteristic of the elements in the sample, EFTEM can be used for elemental/chemical mapping. It can also be used to improve the contrast in images and diffraction patterns by removing inelastically scattered electrons.



9. 3D electron tomography. (S)TEM image is basically 2D projection of 3D object. A special tomography holder is used for tilting sample over a wide angular ranges (for example, -70 degrees to +70 degrees). 2D projection images are taken at each tilting angles. Hundreds of 2D images are aligned and reconstructed to 3D visualization of the imaged object by using backprojection methods. In addition, STEM-EDS tomography can provide chemical information in 3D morphology.

2.3.3 Atomic force microscopy (AFM)

Atomic force microscopy (AFM) or scanning force microscopy (SFM) is a very-high-resolution type of scanning probe microscopy (SPM), with demonstrated resolution on the order of fractions of a nanometer, more than 1000 times better than the optical diffraction limit. An AFM generates images by scanning a small cantilever over the surface of a sample. The sharp tip on the end of the cantilever contacts the surface, bending the cantilever and changing the amount of laser light reflected into the photodiode. The height of the cantilever is then adjusted to restore the response signal, resulting in the measured cantilever height tracing the surface. An atomic force microscope on the left with controlling computer on the right.

Atomic force microscopy (AFM) is a type of scanning probe microscopy (SPM), with demonstrated resolution on the order of fractions of a nanometer, more than 1000 times better than the optical diffraction limit. The information is gathered by "feeling" or "touching" the surface with a mechanical probe. Piezoelectric elements that facilitate tiny but accurate and precise movements on (electronic) command enable precise scanning. Despite the name, the Atomic Force Microscope does not use the Nuclear force.

2.3.4 Wettability

Wettability is the ability of a liquid to maintain contact with a solid surface.

1] Contact Angle : A contact angle (also referred to as a wetting angle) is formed when a drop of liquid is placed on a material surface. The surface tension of the liquid and the attraction of the liquid to the surface causes the drop to form a dome shape. If the drop is small and the surface tension of the liquid is high, it will form a perfect hemisphere. The point where the perimeter of a liquid drop, the liquid-solid interface, and the solid all meet is called the three-phase contact point. The contact angle is defined as the angle between a tangent to the liquid surface and the solid surface at this point. θ is the contact angle in the illustration above. If the drop of liquid spreads across a surface, the contact angle becomes smaller. If the drop of liquid beads up on the surface (as you might see with a



drop of water on a water-resistant article of clothing or a waxed car), the perimeter of the drop retracts, and the contact angle becomes larger.

The contact angles that form depend on several things, including the thermodynamic properties of the liquid and the surface, the way the liquid is brought into contact with the surface, whether there is any time-dependent interaction of the liquid and solid surface, and (for relatively rough surfaces) on the surface topography.



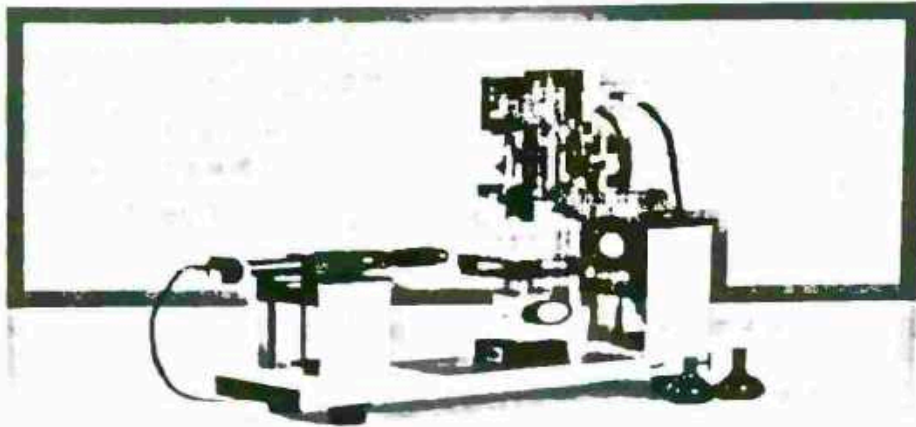
Figure 6 : Low contact angle ;High surface energy and High contact angle;low surface energy.

2] Optical Contact Angle: The optical contact angle measuring and contour analysis systems of the OCA series are high precision optical measuring devices for the measurement of interfacial parameters and phenomena.

The optical analysis of drops that hang from a dosing needle or are placed on a solid surface facilitates the determination of different surface and interfacial parameters. The contact angle that a liquid drop establishes on a solid surface behaviour with said liquid. Having measured the characterises the solid's wetting contact angles of multiple test liquids the surface energy of the solid can be determined and the latter can be used to calculate the work of adhesion for different liquids.

The reliable and experimentally robust measurement of the contact angle aids on the development of surface coatings, composite materials, paints and varnishes or cleaning agents. In short: the measurement of contact angle helps in all situations where solids and liquids meet and advantage is to be gained by the control of wetting and adhesion properties.



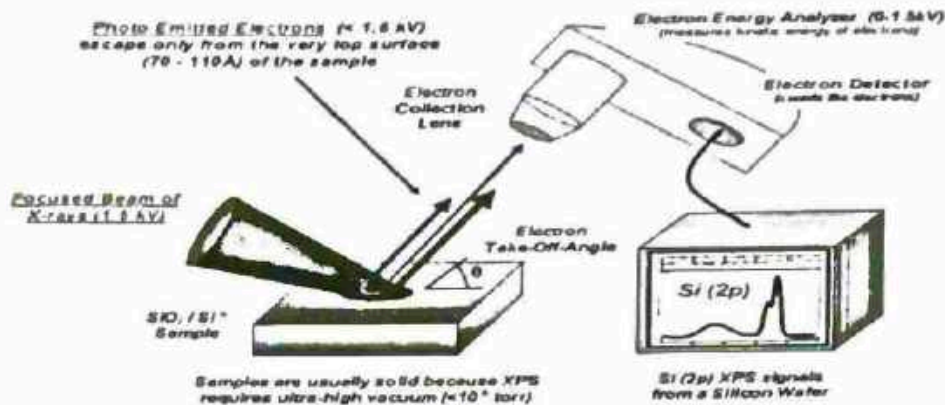


3] Angle of Sliding : The sliding angle is a measure of the mobility of a drop on the surface, which is of concern to a variety of applications from textiles to microfluidics.

The sliding angle SA is the tilt angle TA at which the movement of the drop across the surface begins. The dynamic contact angle is the contact angle during the wetting (advancing angle θ_{Adv}) and dewetting (receding angle θ_{Rec}) processes, i.e. during the movement of the drop across the surface.

4] X-ray photoelectron spectroscopy : X-ray photoelectron spectroscopy (XPS) is a surface-sensitive quantitative spectroscopic technique based on the photoelectric effect that can identify the elements that exist within a material (elemental composition) or are covering its surface, as well as their chemical state, and the overall electronic structure and density of the electronic states in the material. XPS is a powerful measurement technique because it not only shows what elements are present, but also what other elements they are bonded to. The technique can be used in line profiling of the elemental composition across the surface, or in depth profiling when paired with ion-beam etching. It is often applied to study chemical processes in the materials in their as-received state or after cleavage, scraping, exposure to heat, reactive gasses or solutions, ultraviolet light, or during ion implantation.





XPS belongs to the family of photoemission spectroscopies in which electron population spectra are obtained by irradiating a material with a beam of X-rays. Chemical states are inferred from the measurement of the kinetic energy and the number of the ejected electrons. XPS requires high vacuum (residual gas pressure $p \sim 10^{-6}$ Pa) or ultra-high vacuum ($p < 10^{-7}$ Pa) conditions, although a current area of development is ambient-pressure XPS, in which samples are analyzed at pressures of a few tens of millibar.

When laboratory X-ray sources are used, XPS easily detects all elements except hydrogen and helium. The detection limit is in the parts per thousand range, but parts per million (ppm) are achievable with long collection times and concentration at top surface.

XPS is routinely used to analyze inorganic compounds, metal alloys, polymers, elements, catalysts, glasses, ceramics, paints, papers, inks, woods, plant parts, make-up, teeth, bones, medical implants, bio-materials, coatings, viscous oils, glues, ion-modified materials and many others. Somewhat less routinely XPS is used to analyze the hydrated forms of materials such as hydrogels and biological samples by freezing them in their hydrated state in an ultrapure environment, and allowing multilayers of ice to sublime away prior to analysis.



2.4 References

- [1] R.K. Gupta, G.J. Dunderdale, M.W. England, A. Hozumi, Oil/water separation techniques: a review of recent progresses and future directions, *J. Mater. Chem. A* 5 (31) (2017) 16025–16058.
- [2] S.S. Lathe, C. Terashima, K. Nakata, M. Sakai, A. Fujishima, Development of sol-gel processed semi-transparent and self-cleaning superhydrophobic coatings, *J. Mater. Chem. A* 2 (15) (2014) 5548–5553.
- [3] Nicolas Verplanck, Yannick Coffinier, Vincent Thomy, Rabah Boukherroub
Wettability Switching Techniques on Superhydrophobic Surfaces (2007) 577-597
- [4] <https://www.sciencedirect.com/topics/engineering/surface-characterization-technique>
- [5] 0
- [6] Shirtcliffe, N.J., et al. (2007) Superhydrophobic to Superhydrophilic Transitions of Sol-Gel Films for Temperature, Alcohol or Surfactant Measurement. *Materials, Materials Chemistry and Physics*, 103, 112-117.





Experimental Research Work



CHAPTER 3
EXPERIMENTAL RESEARCH WORK

3.1		Introduction
3.2		Experimental work
	3.2.1	Chemicals used
	3.2.2	Preparation of superhydrophobic sponge
	3.2.3	Detailed procedure
	3.2.4	Oil water separation
3.3		Characterization
3.4		Result and Discussion
	3.4.1	Water contact angle
	3.4.2	Mechanical durability
	3.4.3	UV illumination study
	3.4.4	Oil water separation
3.5		References



Chapter 3

3.1 Introduction

Superhydrophobic coatings have garnered significant attention due to their ability to repel water and resist wetting. The unique properties of superhydrophobic surfaces, such as high water contact angles and low contact angle hysteresis, have found applications in a wide range of fields, including self-cleaning surfaces, anti-icing coatings, and microfluidic devices. Sponges, with their porous and highly absorbent nature, present an intriguing substrate for the deposition of superhydrophobic coatings. Various methods have been developed to prepare superhydrophobic coatings on sponges, each offering distinct advantages and tailored for specific requirements. These methods encompass a diverse range of techniques. Each method employs different strategies to achieve the desired superhydrophobic properties on the sponge surface. The selection of an appropriate method for the preparation of superhydrophobic coatings on sponges depends on several factors, including the substrate material, desired coating thickness, roughness control, and the availability of specific chemicals and equipment. The ultimate goal is to create a durable and robust superhydrophobic coating that exhibits exceptional water repellency and self-cleaning properties while maintaining the underlying structure and functionality of the sponge material.

3.2 Experimental Work

3.2.1 Chemicals Used :-

- 1) Chloroform(CHCL₃) M.W 119.3
- 2) Polystyrene 192000M.W
- 3) Polyurethane sponges(P D Industries)
- 4) Candle-soot(CS)

3.2.2 Preparation of superhydrophobic sponge

3.2.1 Dip Coating

During the dip coating process, the sponge was immersed vertically in a solution containing candle soot and polystyrene. However, it was noticed that during the initial dipping cycles, the candle soot tended to settle down after some time. Specifically, it was observed that the candle soot particles were predominantly adsorbing at the bottom of the sponge. In order to achieve a uniform and homogeneous solution, the mixture was stirred during each dipping cycle. This stirring action ensured that the candle soot particles were evenly dispersed throughout the solution, resulting in a uniform coating on the sponge. To facilitate the adsorption of particles onto the sponge's surface, the sponge was carefully immersed in the solution and slowly removed



Chapter 3

by hand. This slow speed allowed for a gradual attachment of particles onto the sponge, enhancing the coating process.

3.2.2 Detailed procedure of preparation of superhydrophobic sponge

◆ Collection of candle soot

To collect candle soot, a metal plate or box was positioned in the central region of the candle flame, allowing the soot to accumulate. Subsequently, the collected candle soot was dissolved in an appropriate quantity of chloroform and filtered through a sponge with a pore size of 50 nm. This filtration process ensured that the resulting solution contained carbon nanoparticles smaller than 50 nm. The filtered solution was then gently heated on a hotplate, maintaining a temperature of approximately 40°C, to facilitate the evaporation of chloroform. This step yielded carbon nanoparticles in their isolated form, ready for subsequent processing and utilization in further applications.

◆ Deposition on sponge

The first step involved dissolving polystyrene in chloroform, and the mixture was stirred using a magnetic stirrer for thirty minutes. After this initial stirring, candle soot was introduced into the same solution, and the stirring process was continued for an additional thirty minutes. The amount of candle soot added was varied during the experiments. Once the solution was prepared, the next step was to dip the sponge into the solution. Below is a schematic representation of the procedure:

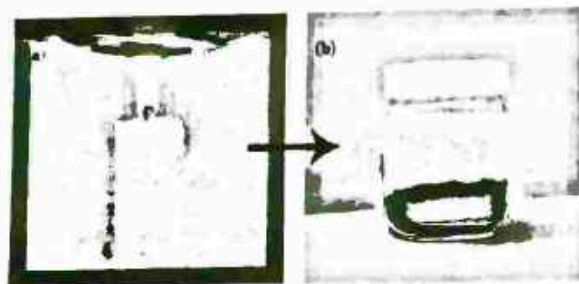


Figure 1: Preparation of candle soot.



Figure 2: Schematic representation of deposition on sponge.



Chapter 3

The deposition was taken for the fixed time interval for varying candle soot quantity. The variations are summarised in the following table.

Table 1 : Summary of work with varying candle soot and deposition time.

Sr. No.	Sample code	Candle soot in mg	Polystyrene in mg	Chloroform in ml	Deposition time in min
1	M1	400	1000	50	5
2	M 2	400	1000		10
3	M 3	600	1000		5
4	M 4	600	1000		10
5	M 5	500	1250		5
6	M 6	500	1250		10
7	M 7	600	1500		5
8	M 8	600	1500		10
9	M 9	450	900		5
10	M 10	350	800		5

3.2.3 Oil-Water Separation.

The absorption separation process of oil from oil-water mixture by superhydrophobic modified sponge is shown in Figure 3. The oil-water mixture was prepared by adding 10 ml oil in 40 ml water. Three types of oils such as diesel, kerosene, and petrol were used to study the oil-water separation. The superhydrophobic sponge was dipped in oil-water mixture and it was observe that superhydrophobic sponge quickly absorbed oil in few seconds. The oil-absorbed sponge was pulled up and squeezed in another beaker to collect oil. Figure 3 depicts optical images of absorption and squeezing process of sponge. The oil-water separation ability of superhydrophobic sponge was tested by using lubricant oil . So, this promising, facile, and energy-saving method can be used to remove the oil from oil-contaminated area.



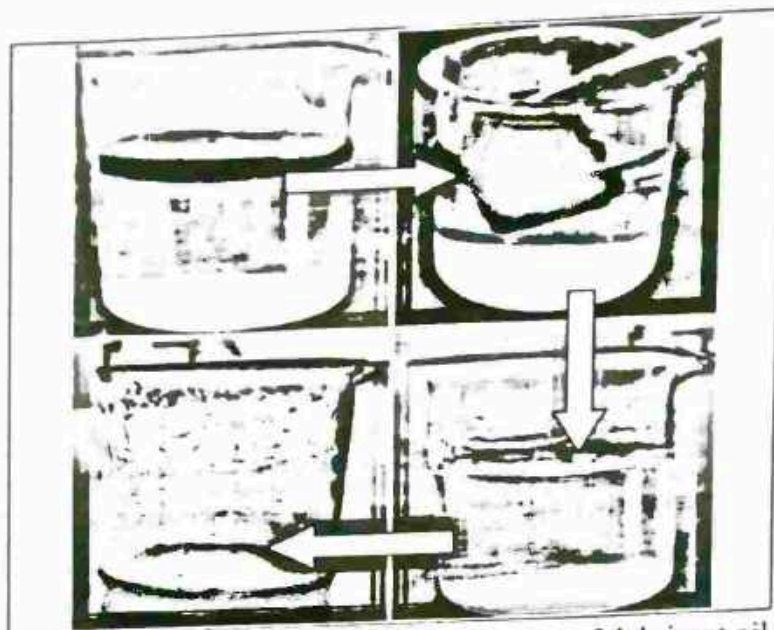
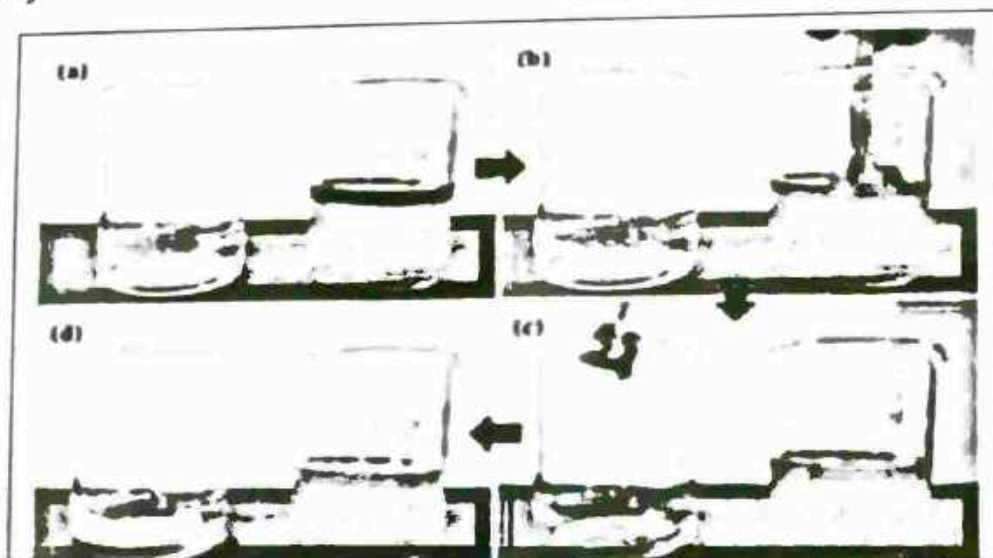


Figure 3 : Optical images of process of removal and collection of lubricant oil from oil-–water separation

In another way, the oil removal ability of sponge was tested using mixture of oil and muddy water. The muddy water was prepared by adding 10 g soil in 50 mL water by stirring. Five milliliter kerosene was added in muddy water and stirred well to mix oil in it. After few seconds, a layer of oil surfaced on muddy water. The oil was removed from muddy water by simply dipping superhydrophobic sponge in the oil-muddy water mixture (Figure 4). The porous structure superhydrophobic sponge was able to absorb oil and repel muddy water completely.



Chapter 3

Figure 4: Optical images of removal and collection of oil from the mixture of oil-muddy water by P3 sample.

3.3 Characterization

3.3.1 Water contact angles

The contact angles of water were determined using a contact angle meter (HO-1AIXCAM-01, Holmarch Opto-Mechatronics Pvt. Ltd. India). These contact angles provided insights into the wetting characteristics of the coated sponge. An increase in the water contact angle indicated an enhanced water-repellent property or increased hydrophobicity of the surface. To measure the contact angles, water droplets were carefully placed at various positions on the surface of the coated sponge. By analyzing the contact angles at different locations, the average contact angle was calculated to minimize potential errors in the measurements.

3.3.2 Mechanical durability

The mechanical durability of the coated sponge is a critical factor that is assessed through an adhesive test. This test helps evaluate the strength and stability of the coating's adhesion to the sponge substrate. In the adhesive test, a controlled force or stress is applied to the coated sponge surface using specific methods such as tape peeling, abrasion, or rubbing. The objective is to examine the ability of the coating to withstand mechanical stresses and resist detachment or damage. By subjecting the coated sponge to these tests, researchers can gain valuable insights into its durability, which is crucial for its intended applications and long-term performance.

3.3.3 UV illumination study

The UV illumination study of the coated sponge is essential for evaluating its superhydrophobic properties. The coated sponge is exposed to UV light for a specific duration to investigate the stability of the superhydrophobic coating under UV radiation. This study examines potential changes in surface chemistry, surface roughness, and the longevity of the coating's hydrophobicity. By subjecting the coated sponge to UV illumination, researchers gain insights into the durability and performance of the superhydrophobic coating, aiding in the development of long-lasting applications. This study helps ensure that the coated sponge maintains its superhydrophobic characteristics even when exposed to UV light, enabling its effective use in various industries and environments.

3.5 Results and Discussion

3.1 Water contact angles

In order to evaluate the hydrophobicity of the coated sponge, an investigation was conducted by varying the quantity of candle soot used during the coating process. Water droplets were carefully placed on the surface of the coated sponges, and the resulting contact angles were



Chapter3







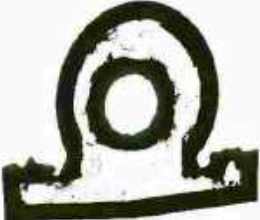



measured visually. The study involved three different quantities of candle soot . The contact angles of water on these coated sponges were determined and recorded, and the data is presented in Table 2

Table 2 : Variation in contact angles with different quantities of candle soot.

Sr no.	Sample code	Contact angles	
		Right angles	Left angles
1	M 1	139.0°	133.0°
2	M 2	134.1°	137.9°
3	M 3	141.5°	134.4°
4	M 4	120.6°	127.9°
5	M 5	127.1°	115.8°
6	M 6	130.9°	147.2°
7	M 7	141.8°	132.0°
8	M 8	141.5°	125.1°
9	M 9	143.7°	145.8°
10	M 10	151.5°	154.6°



Chapter 3

Sample code	Contact angles figure	Sample code	Contact angles figure
M 1		M 6	
M 2		M 7	
M 3		M 8	
M 4		M 9	
M 5		M 10	



Chapter 3

The observed contact angles demonstrate the impact of the candle soot quantity on the hydrophobic properties of the coated sponge. As the amount of candle soot increased, the contact angle also increased, indicating enhanced hydrophobicity. The increasing quantity of candle soot in the coating process enhances the hydrophobicity of the sponge. As the contact angle increases, the surface becomes more water-repellent, which is a desirable characteristic for applications where water resistance is crucial. These findings provide valuable insights into the optimization of the coated sponge for superhydrophobic applications. By understanding the relationship between the quantity of candle soot and the resulting hydrophobic properties, researchers can fine-tune the coating process to achieve the desired level of water repellency.

3.2 Mechanical durability

The mechanical durability of the coated sponge is often evaluated using an adhesive tape test. This specific test is designed to assess the adhesion strength and stability of the coating on the sponge substrate. The adhesive tape test provides valuable insights into the coating's ability to withstand mechanical stresses and resist detachment. In the adhesive tape test, a piece of adhesive tape with known adhesive strength is firmly applied to the surface of the coated sponge. The tape is then quickly peeled off at a specific angle and speed, exerting a controlled force on the coating.

The objective is to evaluate how well the coating adheres to the sponge and whether it remains intact or exhibits signs of detachment or damage. After the tape is removed, a visual inspection is conducted to assess the coating's condition. The researchers carefully examine the tape and the surface of the sponge to detect any signs of coating failure, such as partial or complete detachment, cracks, or peeling. The extent of damage or detachment is recorded and analyzed to quantify the adhesion strength of the coating.

The adhesive tape test serves as a reliable indicator of the coating's mechanical durability. It helps determine the coating's ability to withstand stress, abrasion, or rubbing, which are common mechanical challenges in real-world applications. The results of the The observed contact angles demonstrate the impact of the candle soot quantity on the hydrophobic properties of the coated sponge. As the amount of candle soot increased, the contact angle also increased, indicating enhanced hydrophobicity. This figure illustrates the variation in contact angles for the different quantities of candle soot. The plotted points show the relationship between the candle soot quantity and the resulting contact angles, highlighting the trend of increasing contact angles with increasing candle soot content. The data in Table 3. collectively indicate that increasing the quantity of candle soot in the coating process enhances the hydrophobicity of the sponge. As the contact angle increases, the surface becomes more water-repellent, which is a desirable characteristic for applications where water resistance is crucial.

These findings provide valuable insights into the optimization of the coated sponge for superhydrophobic applications. By understanding the relationship between the quantity of candle soot and the resulting hydrophobic properties, researchers can fine-tune the coating process to achieve the desired level of water repellency.



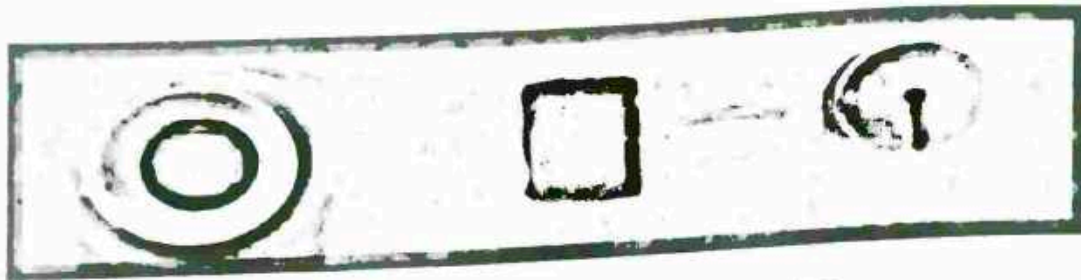


Figure 5: The mechanical durability test setup.

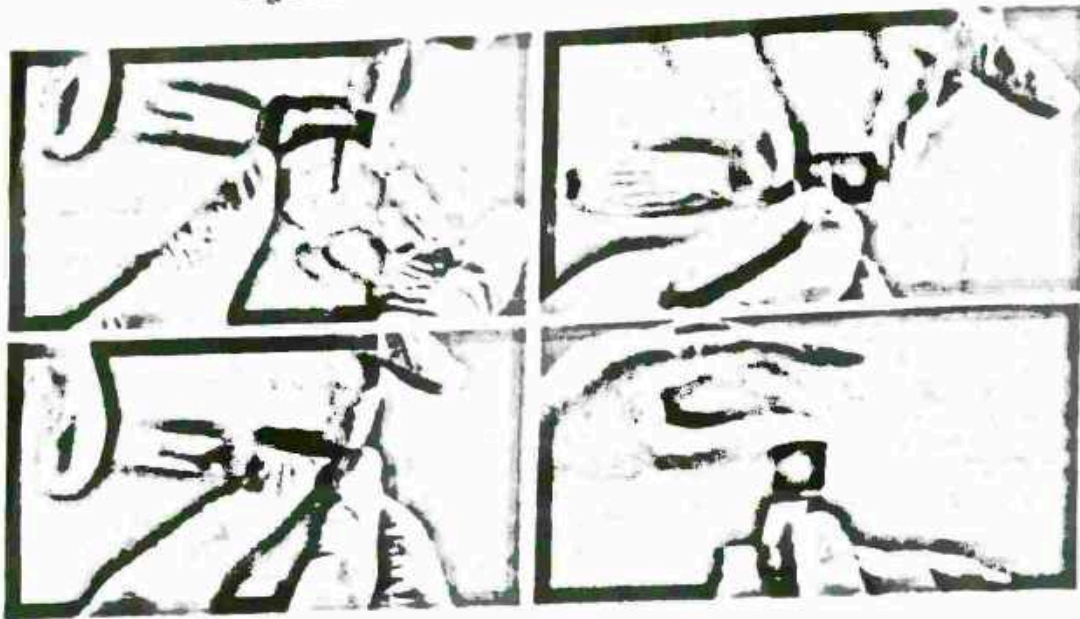


Figure 6: The mechanical durability of the coated sponge is often evaluated using an adhesive tape test.

During the evaluation of the coated sponge using an increasing number of adhesive tape Tests, an interesting trend was observed in the contact angles of water for the M9 sample. The contact angles decreased progressively as the number of adhesive tape tests increased. Initially, the M9 sample exhibited a water contact angle of 145.8° before any adhesive tape tests were conducted. However, after subjecting the coated sponge to a 10 adhesive tape tests, the contact angle decreased to 124.6° . This significant reduction in contact angle indicates a decrease in the hydrophobicity of the surface.



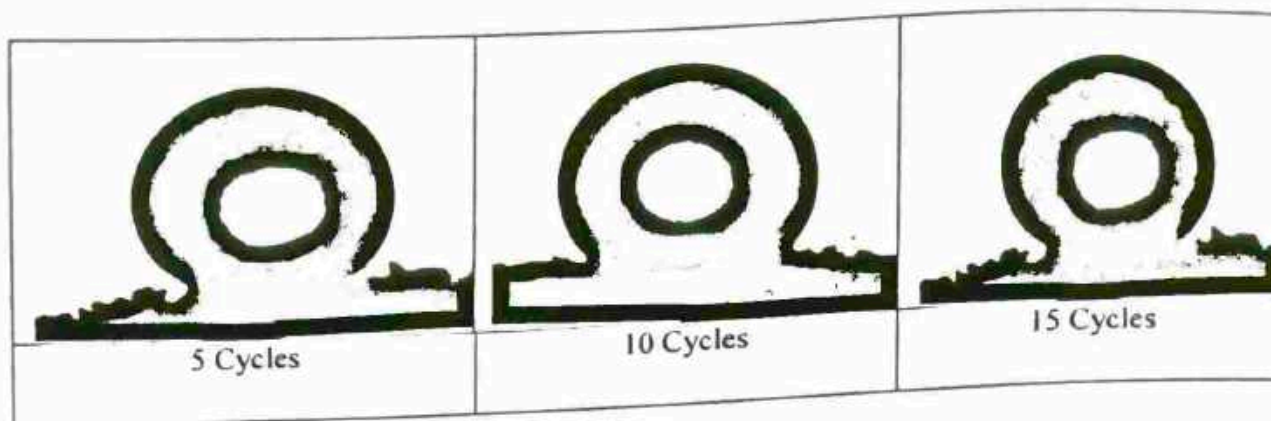


Figure 7: Variation in the contact angles with increasing number of adhesive tape test for M9 Sample

Table 3 : Variation in contact angles with increasing number of adhesive tape test for M9 sample.

Sr no	Number of adhesive tape test	Contact angle
1	5	145.8°
2	10	122.4°
3	15	124.6°

The observed decrease in contact angles can be attributed to the mechanical stress exerted by the adhesive tape during the tests. As the tape is peeled off from the surface, it applies a shearing force that can potentially disrupt the integrity of the coating. This disruption may lead to the formation of microcracks or the removal of the hydrophobic components, resulting in decreased water repellency.

The reduction in contact angles suggests a compromised hydrophobic surface and a potential decrease in the coating's durability. The repeated application and removal of the adhesive tape might have gradually weakened the adhesion of the coating to the sponge substrate, leading to the observed loss in hydrophobicity.

These findings highlight the importance of considering the mechanical durability of the coated sponge when assessing its performance in real-world applications. While the initial contact angle of 145.8° indicated a promising level of hydrophobicity, the decrease to 124.6° after 10 adhesive tape tests raises concerns about the long-term effectiveness of the coating under mechanical stress.

2.3.3 UV illumination study

Conducting a UV illumination study on the coated sponge is crucial for assessing its superhydrophobic properties. This study involves subjecting the coated sponge to UV light for a specific duration to examine the stability of the superhydrophobic coating under UV radiation. The primary objective is to investigate potential changes in surface chemistry, surface roughness, and the longevity of the coating's hydrophobicity.



The UV illumination study provides valuable insights into the durability and performance of the superhydrophobic coating. UV radiation can have a significant impact on surface properties, including the degradation of coatings and alterations in surface chemistry. By exposing the coated sponge to UV light, researchers can observe any changes in its hydrophobic characteristics over time and evaluate the coating's resistance to UV-induced degradation.

This study helps ensure that the coated sponge maintains its superhydrophobic properties even when exposed to UV light, which is essential for its effective use in various industries and environments. Understanding the behavior of the coating under UV illumination is crucial for applications that involve outdoor exposure or UV-rich environments, such as construction, automotive, or aerospace industries. During the UV illumination study, various parameters can be monitored and analyzed, including changes in contact angles, water droplet behavior, surface roughness measurements, and surface chemistry analysis. These evaluations provide valuable data on the performance and longevity of the superhydrophobic coating, enabling researchers to optimize the coating formulation or application process to enhance its UV resistance.

By gaining insights into the durability of the superhydrophobic coating under UV illumination, researchers can develop long-lasting applications that maintain their hydrophobic properties over extended periods. This ensures the effectiveness and reliability of the coated sponge in real-world scenarios, where exposure to UV light may be inevitable.

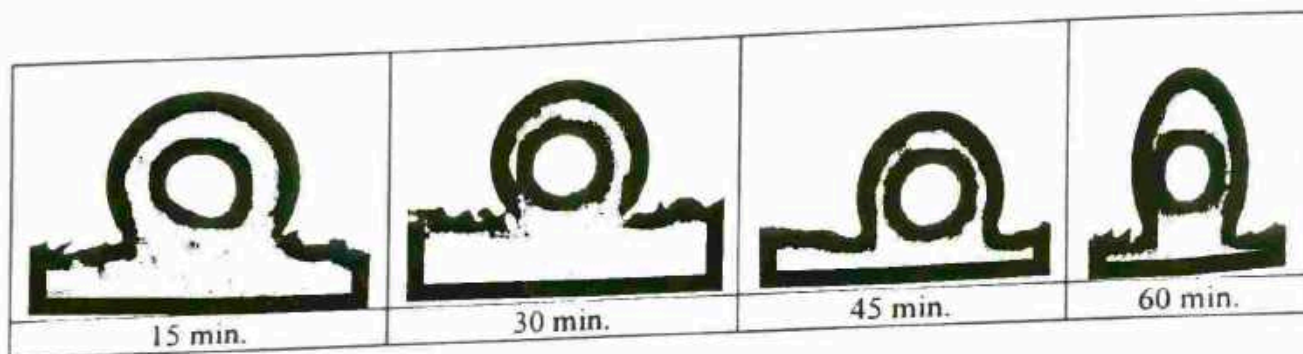


Figure 7: Variation in the contact angles with increasing UV illumination time.

Table 4 : Variation in contact angles with increasing UV illumination time.

Sr.No.	UV illumination time (minutes)	Contact angles
1	15	101.1°
2	30	125.7°
3	45	112.4°
4	60	129.0°

This study presents the relationship between UV illumination time and the resulting contact angle of the coated sponge. The contact angles were measured at different time intervals, ranging from 15 to 60 minutes of UV exposure.

It is observed that as the UV illumination time increases, there is a gradual increase in the contact angle of the coated sponge. At the initial UV exposure time of 0 minutes, the contact angle is measured at 99°. As the UV exposure time increases to 15, 30, 45, and 60 minutes, the



Chapter 3

contact angles progressively increase to 101.1°, 125.7°, 112.4°, and 129°, respectively. This trend suggests that the UV illumination has an influence on the surface characteristics and hydrophobicity of the coated sponge. The gradual increase in contact angle indicates an enhancement in the water repellency of the surface as the UV exposure time increases.

2.3.4 Oil - Water – Separation.

An oil water separator is a piece of equipment used to separate oil and water mixtures into their separate components. There are many different types of oil-water separator. Each has different oil separation capability and are used in different industries.

For oil water separation we used sample M10. The deposition sponge weight is 0.239 gm and the weight after oil absorption is 6.480 gm. The result is that the absorption capacity is 26.11gm.



4.1 References

Chapter 3

[1] Celia, E., Darmanin, T., de Givenchy, E. T., Amigoni, S., & Guittard, F., "Recent advances in designing superhydrophobic surfaces", *Journal of colloid and interface science*, 402, 1-18, 2013.

[2] Li, X. M., Reinhoudt, D., & Crego-Calama, M., "What do we need for a superhydrophobic surface? A review on the recent progress in the preparation of superhydrophobic surfaces" *Chemical Society Reviews*, 36(8), 1350-1368, 2007.

[3] Xue, C. H., Zhang, Z. D., Zhang, J., & Jia, S. T., "Lasting and self-healing superhydrophobic surfaces by coating of polystyrene/SiO₂ nanoparticles and polydimethylsiloxane", *Journal of Materials Chemistry A*, 2(36), 15001-15007, 2014.

[4] Yuan, S., Strobbe, D., Kruth, J. P., Van Puyvelde, P., & Van der Bruggen, B., "Superhydrophobic 3D printed polysulfone membranes with a switchable wettability by self-assembled candle soot for efficient gravity-driven oil/water separation", *Journal of Materials Chemistry A*, 5(48), 25401-25409, 2017.



Chapter 4

Conclusion



Chapter 4

Conclusion

To address the persistent issue of oil leakages and spills, we have developed a simple yet effective method to separate oil from oil-water mixtures. Our approach capitalizes on the hydrophobic properties of candle soot, utilizing it in conjunction with a porous surface specifically, a sponge. By coating and modifying the sponge with candle soot and polystyrene, we have successfully enhanced its ability to repel water and attract oil. The quantity of candle soot used in the coating process plays a significant role in determining the hydrophobicity of the sponge. Through our experiments, we observed that increasing the amount of candle soot resulted in higher contact angles and improved water repellency. While the hydrophobic coating demonstrates commendable performance, it is crucial to consider the mechanical durability of the coated sponge. We conducted adhesive tape tests to assess the coating's ability to withstand mechanical stress. The results revealed a decrease in the contact angle from 145.8° to 124.6° after ten tests, indicating potential limitations in the coating's long-term effectiveness under mechanical strain. In addition to mechanical durability, we also investigated the impact of UV illumination on the coated sponge. Our study revealed a positive relationship between UV exposure time and the contact angle of the coated sponge. As the duration of UV illumination increased, the contact angles progressively rose, indicating an enhancement in the hydrophobic properties of the coating. However, to determine the optimal UV exposure time and evaluate the long-term stability and durability of the coating's hydrophobicity under UV radiation, further investigations are required. Overall, our research showcases a promising approach for separating oil from oil-water mixtures using a modified sponge coated with candle soot and polystyrene. The quantity of candle soot, mechanical durability, and UV exposure time all have significant impacts on the performance of the coated sponge. By addressing these factors through ongoing studies, we can refine the coating process and advance the development of effective solutions for oil spill remediation and water purification applications.



Fabrication of Superhydrophobic Polycarbonate Substrate By Using Template Method.

A Dissertation Report submitted to



Vivekanand College (Autonomous), Kolhapur.

For the Partial Fulfillment of
Degree of Master of Science
In

PHYSICS
Under the faculty of Science

By

Miss. Priyanka Balaso Khot
B.Sc. Physics

Under the Guidance of
Dr. S.S. Latthe (M.Sc. Ph.D)

Department of Physics
Vivekanand College (Autonomous), Kolhapur

2022-2023



DECLARATION

I hereby declare that, the project entitled "**Fabrication of superhydrophobic polycarbonate substrate by template method**" completed and written by me has not previously formed the basis for the award of any Degree or Diploma or other similar title of this or any other University or examining body.

Place: Kolhapur

Date: 27/05/2023



Priyanka Khot

B.Sc Physics



CERTIFICATE

This is to certify that the project entitled “ **Fabrication of superhydrophobic polycarbonate substrate by template method**” which is being submitted here with for the award of the Degree of Master of Science in Physics of Vivekanand College (Autonomous), Kolhapur, is the result of the original project work completed by Priyanka Balaso Khot. under our supervision and guidance and to the best of our knowledge and belief the work embodied in this project has not formed earlier the basis for the award of any Degree or similar title of this or any other University or examining body.

Place: Kolhapur

Date: 27/05/2023


Project Guide


Examiner


Head

Department Of Physics
HEAD
DEPARTMENT OF PHYSICS
VIVEKANAND COLLEGE, KOLHAPUR
(AUTONOMOUS)



ACKNOWLEDGEMENT

On the day of completion of this project, I offer sincere gratitude to those who encouraged and helped me a lot at various stages of this work. I have great pleasure to express my deep sense of indebtedness and heart full gratitude to Dr.S.S. Lathe e, Professor, Department of Physics, Vivekanand College (Autonomous), Kolhapur, for his expert and valuable guidance and continuous encouragement given to me during the course of my project work. He has already been a source of strength for me. I find in him a real researcher who through his own example and devotion for scientific work inspired me towards a common goal of achieving scientific knowledge and pursuit. I wish to express my appreciation to Prof. S.V. Malgaonkar, Prof. C.J. Kamble, and Prof. G.J. Navathe for discussion and co-operation in each and every movement of my project work.

My acknowledgement will be incomplete if I don't express my appreciation towards my family members whose good will & inspiration helped us a lot in completing this project work.

Priyanka

Priyanka Balaso Khot

M.Sc – II (Physics)



INDEX

Chapter No.	Contents	Page No.
I	1.1 Introduction of superhydrophobicity 1.2 Basic Principle of Superhydrophobic materials 1.3 Wetting behaviour on a solid surfaces 1.4 Applications	01 -15
II	2.1 Literature Survey 2.2 Fabrication methods 2.3 Characterization Technique	16-39
III	3.1 Introduction 3.2 Experimental 3.3 Characterization 3.4 Result and discussion	40-46
IV	4.1 Conclusion 4.2 Future Plan	47-48



Chapter 1

1. Introduction of Superhydrophobicity

Nature is the biggest 'consultancy centre' in the world, the freely consulting researches who are finding solutions for the scientific problems. Beading of water on the solid surfaces can classify them as 'superhydrophobic'.

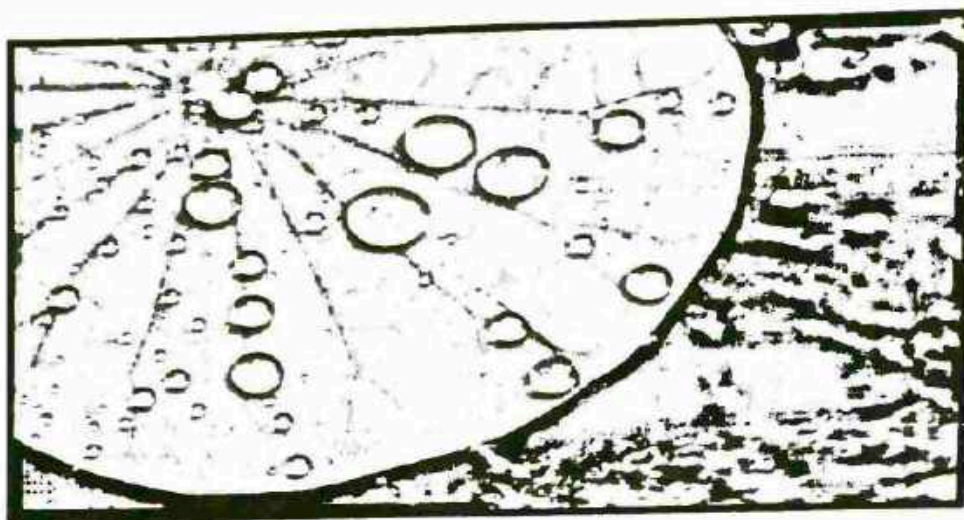


Fig 1 superhydrophobic

"Superhydrophobicity" was first observed in lotus leaf and in some other plants in which their leaves would not get wet. The main reason of this phenomenon was the unique surface structure of the lotus leaf and presence of low surface energy material on the surface of leaf. In order to achieve the superhydrophobic surface or coating, the surface must possess hierarchical micro and nano roughness and low surface energy at the same time. Hierarchical micro and nanoscale roughness that will trap air on the surface that will cause increase on water contact angle, and low surface energy will decrease the tendency of water to have bonding the surface. So, the almost achieve the superhydrophobicity.



1.1 Inspiration from Nature –

No artificial things can excel the whimsy of nature. Nature is the greatest university, providing all kinds of wonderful things for us. Among them, the special wetting behavior is one of the perfect phenomena, including superhydrophobicity and superhydrophilicity. For the natural superhydrophobic surfaces, Neinhuis and Barthlott investigated the characterization and distribution of natural waterproof plants leaves as early as 1996. Furthermore, our group also studied some typical natural superhydrophobic plant leaves in detail in 2007.⁵⁴ The knowledge of superhydrophobicity has gradually been known. Nature has been a source of inspiration for a large number of scientific workers to fabricate superhydrophobic materials due to its great practical applications, for instance, self-cleaning, anticorrosion, drug reduction, antifog, anti-icing, and so on. The materials with special wettability have been described in numerous reports, such as plants leaves (typical lotus leaf),^{4,55,56} rose petals⁵⁷ etc. and others in the Animalia Kingdom like mosquito compound eyes and wings/back/legs of insects. Some typical natural superhydrophobic surfaces are presented. The common features of the above examples are appropriate roughness and low surface energy, leading to superhydrophobicity with a water contact angle higher than 150° . In addition to the common features, there also exist different features between Superhydrophobicity is a phenomenon where the water contact angle on a certain surface is bigger than 150° as well as the sliding angle is less than 5° originating from the surface special structure and the chemical composition. There exist a variety of natural superhydrophobic surfaces such as the typical example of the lotus leaf, wing of the butterfly, eye of the mosquito,⁶ leg of the water strider, and so on.



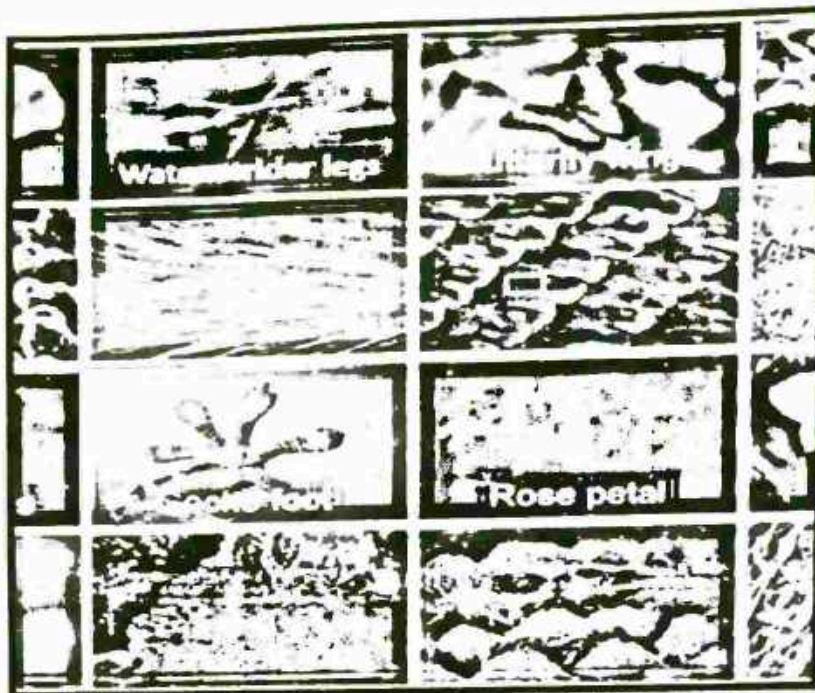


Figure -Superhydrophobic phenomena of interfaces of natural organisms.

1.2 The Basic Principle of Fabricating biomimetic Superhydrophobic Materials

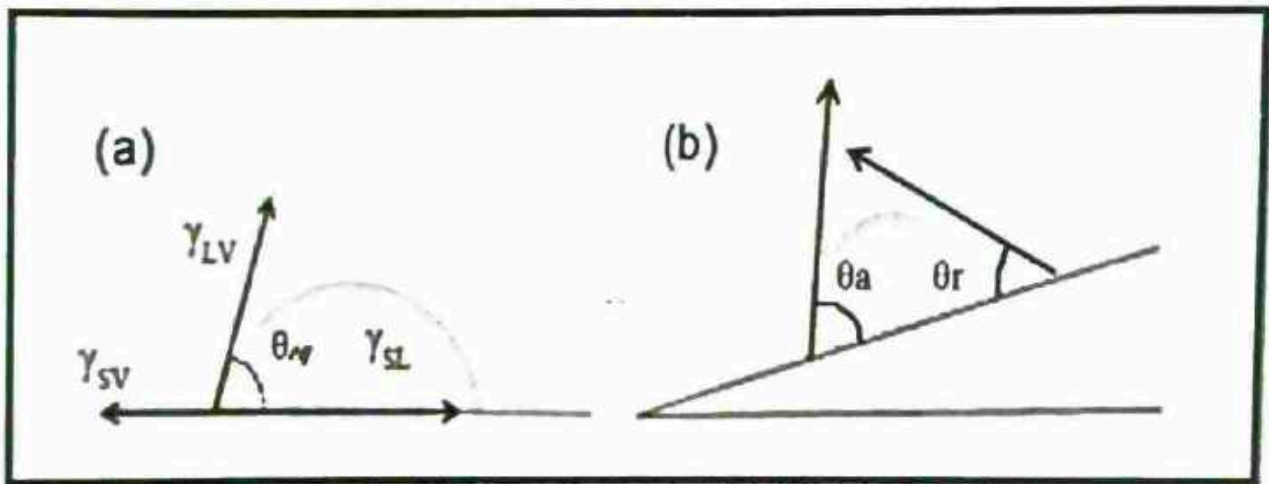
Contact Angle

When a water drop is placed on a flat solid surface, it will form a spherical shape or spread out completely. If the water contact angle is 0° , the drop will spread completely on the flat surface, otherwise it will form a round or flat spherical shape. The contact angle means that the angle that goes through the liquid inside from the solid-liquid interface to the vapor-liquid (Figure 2a). According to the roughness and homogeneity, the contact angle can be classified into Young's contact angle, Wenzel contact angle, and Cassie contact angle. Firstly, on the ideal slippery and the chemical component homogeneous solid surface, the developed contact angle is the equilibrium contact angle, namely Young's contact angle. As shown in Figure 2a, great Thomas Young gave Young's equation that reflects the relationship between the Young's contact angle and the three phase interfacial tensions.

$$\cos \theta = \frac{\gamma_{sv} - \gamma_{sl}}{\gamma_{lv}} \quad \dots\dots\dots (1)$$

Where θ is Young's contact angle; γ_{sv} , γ_{sl} , and γ_{lv} represent the interfacial tensions of solid-vapour, solid liquid, and liquid-vapour, respectively.

The perfectly slippery flat surface is imaginary, although it has a significant value for practical research. All the real surfaces are more or less rough heterogeneously. The drop on these surfaces can be in the stable equilibrium state, or in the metastable state of equilibrium, namely the phenomenon of contact angle hysteresis. Owing to contact angle hysteresis, when the surface is tilted to a certain angle and the drop can be stable on the incline (Figure 2b), the contact angle becomes larger or smaller i.e. advancing angle or receding angle (Figure 2b). If not for the contact angle hysteresis, the water drop will roll off the surface.



F1.2- Schematic illustration of (a) contact angle θ on the flat solid surface and (b) a stable droplet on the tilted surface owing to the contact angle hysteresis, advancing angle θ_a and receding angle (θ_r).

Roughness

Surface roughness can be regarded as the quality of a surface of not being smooth and it is hence linked to human (haptic) perception of the surface texture. From a mathematical perspective it is related to the spatial variability structure of surfaces, and inherently it is a multiscale property.

It has different interpretations and definitions depending from the disciplines considered. Surface roughness, often shortened to roughness, is a component of surface finish (surface texture). It is quantified by the deviations in the direction of the normal vector of a real surface from its ideal form. If these deviations are large, the surface is rough; if they are small, the surface is smooth. In surface metrology, roughness is typically considered to be the high-frequency, short-wavelength component of a measured surface. However, in practice it is often necessary to know both the amplitude and frequency to ensure that a surface is fit for a purpose.

Roughness plays an important role in determining how a real object will interact with its environment. In tribology, rough surfaces usually wear more quickly and have higher friction coefficients than smooth surfaces. Roughness is often a good predictor of the performance of a mechanical component, since irregularities on the surface may form nucleation sites for cracks or corrosion. On the other hand, roughness may promote adhesion. Generally speaking, rather than scale specific descriptors, cross-scale descriptors such as surface fractality provide more meaningful predictions of mechanical interactions at surfaces including contact stiffness and static friction.

Although a high roughness value is often undesirable, it can be difficult and expensive to control in manufacturing. For example, it is difficult and expensive to control surface roughness of fused deposition modelling (FDM) manufactured parts. Decreasing the roughness of a surface usually increases its manufacturing cost. This often results in a trade-off between the manufacturing cost of a component and its performance in application.

Roughness can be measured by manual comparison against a "surface roughness comparator" (a sample of known surface roughness), but more generally a surface profile measurement is made with a profilometer. These can be of the contact variety (typically a diamond stylus) or optical (e.g.: a white light interferometer or laser scanning confocal microscope).

However, controlled roughness can often be desirable. For example, a gloss surface can be too shiny to the eye and too slippery to the finger (a touchpad is a good example) so a controlled roughness is required. This is a case where both amplitude and frequency are very important.

1.3 Wetting behaviour on a solid surface:



The Wetting behaviour of a liquid drop on a solid surface can be experimentally characterized by depositing a liquid drop on the solid surface and measuring contact angle.(figure 1.3)

In general, when the contact angle is less than 90°, the solid surface is considered as 'hydrophillic'; when the contact angle is larger than 90°, the solid surface is considered as 'hydrophobic'. For the lowest surface free energy of the solid-air interface material a contact angle of ~120° has been recorded for water.

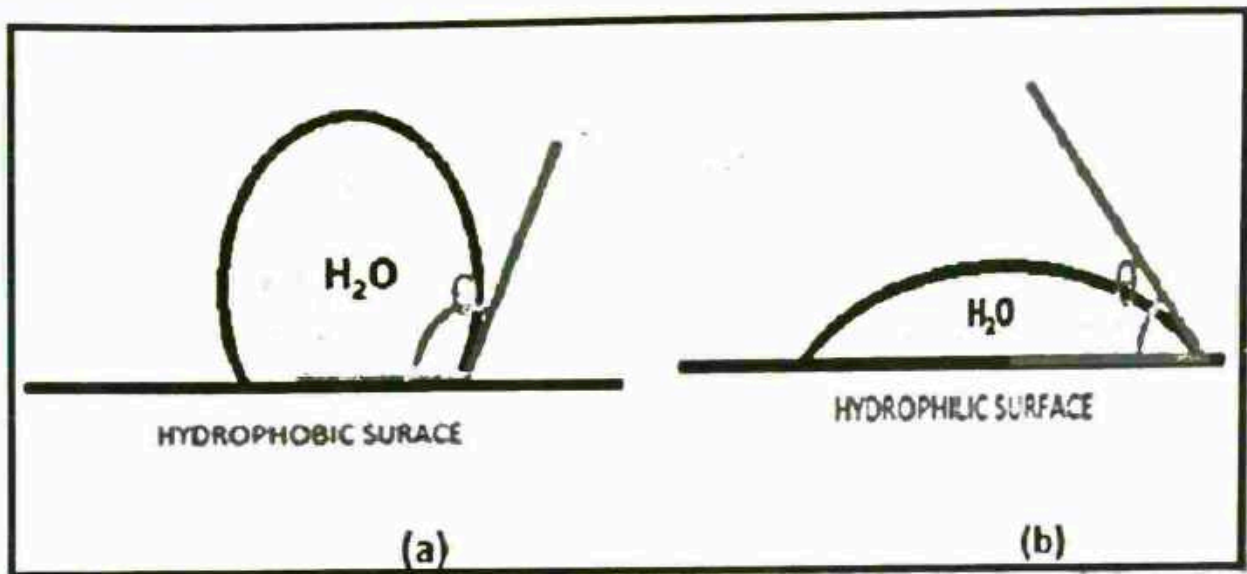


Figure 1.3: (a)- contact angle of a water drop on a hydrophobic surface ; (b)- contact angle of a liquid drop on a hydrophillic surface.

1.3.1 Wetting on a smooth surfaces:

For a smooth and chemically homogeneous solid surface, the contact angle of a water drop can be calculated therotically by the Young's equation,

$$\text{COS } \theta = \frac{Y_{sv} - Y_{sl}}{Y_{lv}} \text{ ----- (1)}$$

Where, Y_{sv} is the solid- vapour interfacial energy. Y_{sl} is the solid- liquid interfacial energy and Y_{lv} is the liquid- vapour interfacial energy. The boundary three phases contact line is schematically Illustrated in Figure

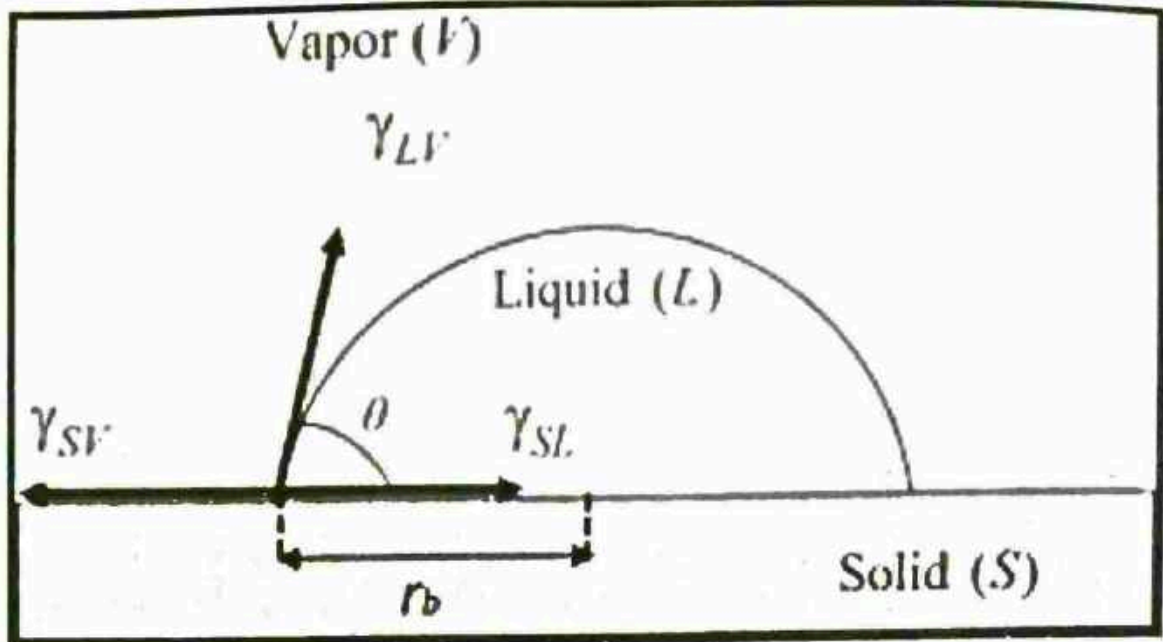


Figure 1.3.1 Sketch of the three phase contact line of a water drop on a solid surface.

The molecules are energetically favourable to be surrounded by other molecules. Compare with The bulk, at the surface, molecules are only partially surrounded by other molecules, this is energetically unfavourable. The energy require to take the molecular from the bulk to the surface to create a new surface is so called "interfacial energy". If the interfacial energy is higher than that of the solid-liquid interface ($\gamma_{sv} > \gamma_{sl}$), the right side of the Young's equation is positive. As a consequence, the value of the contact angle will be in the range of 0° to 90° , which means the liquid partially wet the surface. When the is negative ($\gamma_{sv} < \gamma_{sl}$), the contact angle exceeds 90° , the liquid is said not to wet the solid. Among the three interfacial energies, only can be measured experimentally, using various methods, including capillary rise and pendant drop. No well-established technique exists to measure separately. The Young's Equation only works for flat surface, when the surface become rough, the Young's equation is not suitable anymore.

1.3.2 Wetting on rough surface: Wenzel's and Cassie's model

According to equation (1), the surface hydrophobicity increases with decreasing the surface free energy of the solid-air interface γ_{sv} . Further increase of the hydrophobicity requires manipulation of the surface topography. The fact that roughness can strongly affect the Wetting of a surface was already discussed by Wenzel in 1936 and then by Cassie and Baxter in 1944.

- Wenzel's model

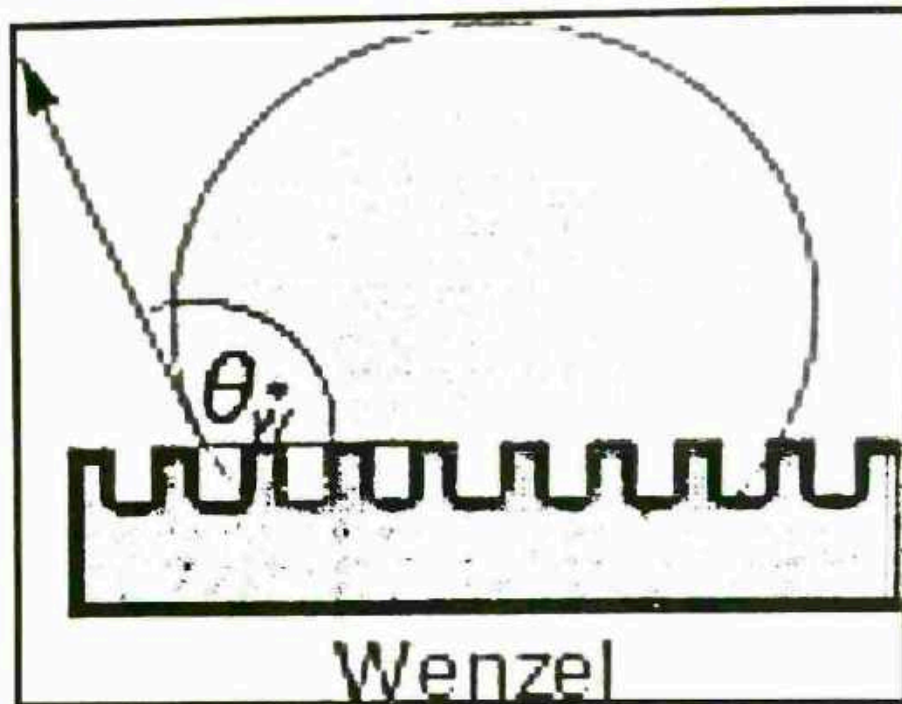


Figure 1.3.2 : Sketch of a water drop on a rough surface in case water penetrates the asperities (Wenzel model).

In the Wenzel state, the drop deposited on a surface and the bottom of the drop penetrates into the asperities (Figure 1.3), the increase of the surface roughness (due to the presence of the texture) amplifies the natural hydrophobicity or hydrophilicity of the material. Thus the key parameter controlling the contact angle on the same material is the solid roughness. The apparent contact angle on such rough surface can be described by the Wenzel equation:

$$\cos \theta_w = r \cos \theta \text{ ----- (2)}$$

where, θ_w is the apparent contact angle, this angle we can observe by eye or an optical microscope; and r defined as the ratio between the true surface area over the projected area, the roughness factor is always larger than 1 for a rough solid surface; θ is the contact angle of the corresponding smooth surface obtained by the Young's equation. For a given hydrophilic surface ($\theta < 90^\circ$), liquid drop has lower contact angle on rough surface compared with corresponding smooth one. If the surface essentially is hydrophobic ($\theta > 90^\circ$), liquid drop has higher contact angle on rough surface compared with corresponding smooth one.

However, Periklis Papadopoulos et al found that the contact angle in Wenzel state is not always the same, if the substrate has regular periodic array. So the pillar distance is different at main axis and diagonal axis. The water contact line pinning at the pillars which has different pillar distance will induce different curvature at the bottom of the drop. The drop shape asymmetry factor is decreasing with increase the distance from the substrate.

Cassie Model

As the surface roughness or the surface hydrophobicity increases, it becomes unlikely for water to completely follow the surface topography of a hydrophobic substrate. Since if water has a complete contact with the solid surface, at this system it is in a high energy state. In the other state, if the water is only partial contact with solid, it is more energy favourable. Instead, air may be trapped between water and the surface texture (Figure 1.4).



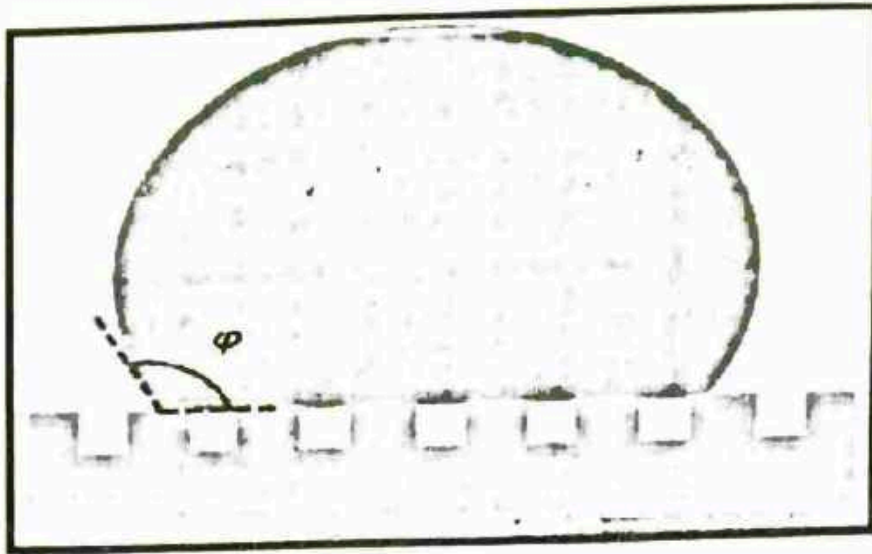


Figure 1.4 A water drop suspended on a rough surface, with air trapped between asperities (Cassie Model).

The apparent contact angle for this vapour-liquid-solid composite interface is the sum from all contributions of the different phase fractions. The minimum interfacial energy, together with Young's relation applied to each solid surface, result to Cassie-Baxter relation:

$$\cos \theta_c = F_1 \cos \theta_1 + F_2 \cos \theta_2 \text{ ----- (3)}$$

Here, θ_c is the apparent contact angle, θ_1 and θ_2 are the contact angles on two different kinds of materials; F_1 and F_2 is the surface fraction of materials 1 and 2, respectively. If the liquid would fully rest on air, the "contact angle" would be 180° : the smaller, the closer to this extreme situation, and the higher the contact angle. More precisely, the contact angle θ_c of such a "fakir" drop is an average between the angles on solid, and on air. For air $\cos(180^\circ) = -1$, and $F_2 = (1 - F_1)$, the equation (3) can be written as follow.

$$\cos \theta_c = F_1(1 + \cos \theta - 1) \text{ ----- (4)}$$

Here represents the solid-liquid fractions under the contact area; is the contact angle on flat surface. This implies for achieve a high apparent contact angle, the contribution from solid phase, should be small as possible.



1.4 Applications -

The continuous development and progress of the superhydrophobic surface not only provide great convenience for daily life but also benefit the sustainable development of resources owing to the properties of gradually optimized superhydrophobic materials such as mechanical stability, anti-abrasion, and self-healing. The excellent superhydrophobic materials are gradually applied to both industries and daily life since applications for biomimetic superhydrophobic surfaces are very important for us, which is the final aim of our research. In this section, it is explained how to modify superhydrophobic materials to bring some attractive functions for us. The main applications of superhydrophobicity are presented including waterproof function, self-cleaning, anti-icing, corrosion resistance, and oil/water separation.

1.4.1 Waterproof Function -

It is obvious that the waterproof function is the basic application of superhydrophobic materials. Based on this primary function, the functional superhydrophobic materials have been extended to other wide applications such as self-cleaning, anti-icing, anticorrosion, and so on. With the technology development and living standards increasing, people's demands on lifestyle products grow even higher. The inherent superhydrophilicity of some materials including cotton, fabrics, paper, and some metals may bring about inconvenience in some practical applications. Amusedly, stable air bubbles present on superhydrophobic surfaces form barriers between the solid surface and the water drop. Thus, the superhydrophobicity provides an effective pathway to protect these sensitive surfaces from being affected by external factors like spilled water, rain etc. For instance, have already fabricated superhydrophobic cotton fabrics. The original good vapour transmissibility and water adsorptivity of the opposite unmodified cotton side were inherited.⁸⁹ this can prevent mildew and extend the scope of cotton applications under moist conditions. Not only can the superhydrophobic surface possess a simple static waterproof function, but the more excellent superhydrophobic surfaces that can resist against the drop water impact have been also obtained via advanced methods. The similar requirements like the above would be addressed to a large extent. The excellent superhydrophobic surfaces of various materials can be applied in different fields like underwater applications and waterproof facilities.

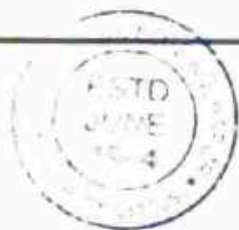
1.4.2 Anti-icing



Ice formation can make some devices difficult to use and bring about the loss of efficiency such as air condition, power lines, and heat exchangers. In addition, ice formation on road can be an inconvenience to the traffic and dangerous for people. A lot of measures have been made to prevent ice formation like an outer insulating layer for high-cold highways.^{21,78,147,148} It has been demonstrated that superhydrophobic surfaces can often prevent or retard ice formation. Recently, Kim et al. successfully achieved superhydrophobic aluminium for effective anti-icing processes. The frosting characteristics were measured by observing the freezing process after comparison with unmodified aluminum at the same condition of freezing, they demonstrate that the obtained superhydrophobic aluminum can contribute to anti-icing applications resulting from the self-propelled jumping motion of the condensate droplets on the surface at a higher saturation. Ice formation can be delayed more than four times under the high saturation of easier freezing. The superhydrophobic surfaces with anti-icing function have wide applications in our daily life including high-cold highway, heat exchangers suffering from freezing problems under cold weather, which is still a challenge for us in how to prolong its anti-icing time with biomimetic superhydrophobic surfaces.

1.4.3 Self-cleaning: Antibacterial, Anti-biofouling, and Antiscaling

The lotus leaf exhibits self-cleaning characteristic owing to superhydrophobicity resulting from the dual-scale hierarchical structure and the chemical composition as well as the low adhesion to the droplet. Accordingly, lotus-like superhydrophobic materials also possess self-cleaning property. The air pockets that are trapped between the water droplet and the nanostructured surface lead to a composite interface formation of solid/air/liquid, thereby allowing the water droplet to immediately roll off simultaneously carrying away the contaminants adhering to the surface. In addition to taking away the contaminants self-cleaning function also include antibacterial, antifouling property and antiscaling functions. Feng et al. investigated the effect of wettability on regulating the bacteria adhesion, which may provide a new insight to create antibacterial materials with extreme wettability. For example, Sun and Wang et al. reported a superhydrophobic surface with Cu/Ag bimetallic composition and hierarchical structure by electrolyses deposition of the porous copper foam (namely replacement reaction) followed by thermal oxidation. For



comparison, they also fabricated a Cu/Ag bimetallic composition from the flat copper alone via the same reaction process. The wettability of the copper surface through silver deposition can be transitioned from hydrophobicity to superhydrophobicity, resulting from the latter thermal oxidation procedure. The oxides on the rough bimetallic composition surface endow the rough surface with low surface energy. In the wet solution, the oxides would release metal ions owing to its higher solubility property together with both hierarchical architecture and bimetallic composition. The release of metal ions makes it antibacterial performance for different applications and hydrophobicity. Recently, durable superhydrophobic and biofouling-resistant steel surfaces were prepared by Aizenberg et al. via electrodeposition. They investigated the anti-biofouling characteristics of the fabricated coatings in the biofouling conditions and demonstrated significantly reduced biofouling of blood staining, *Escherichia coli* attachment, and marine algal adhesion. For antiscaling, taking the research that Jiang et al. reported as the example, they prepared a superhydrophobic surface on the copper substrate, and the antiscaling performance for CaCO_3 has been conformed because the scaling mass per unit area decreased to $0.1607 \text{ mg cm}^{-2}$ from $0.6322 \text{ mg cm}^{-1}$. They mentioned that the antiscaling technology is important to prevent the exchange heater from blocking and the obtained superhydrophobic copper surface with attractive antiscaling performance has great potential applications in practice.



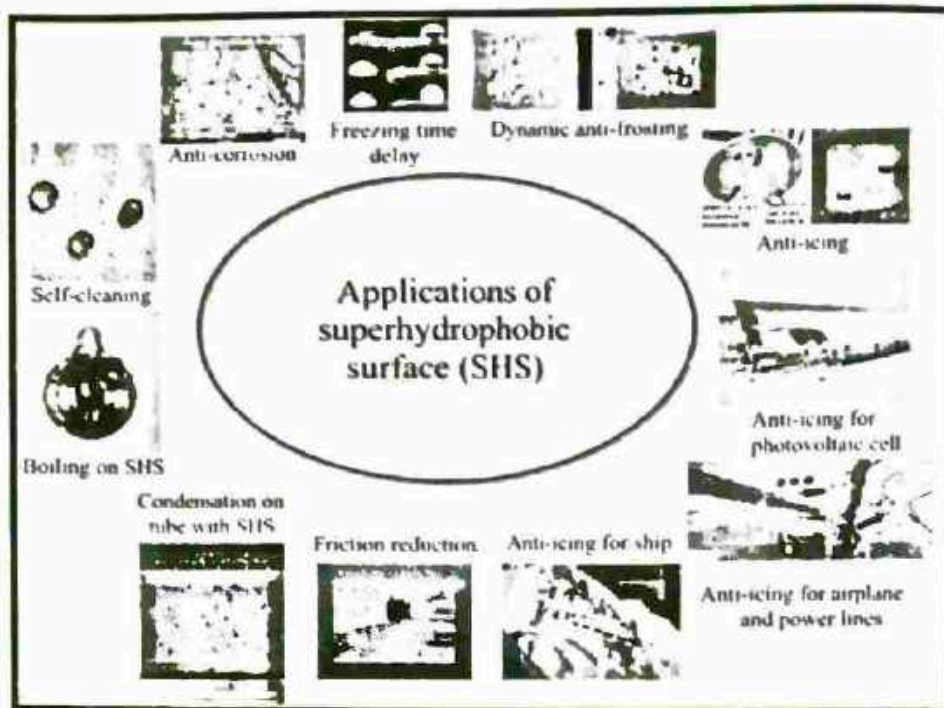


Figure. the properties and corresponding applications of superhydrophobic surfaces.

References

- [1] K. Liu, L. Jiang, Bio-inspired self-cleaning surfaces, *Annu. Rev. Mater. Res.* 42(2012) 231–263.



[2]Wenzel, R. N., RESISTANCE OF SOLID SURFACES TO WETTING BY WATER. *Industrial & Engineering Chemistry* 1936, 28 (8), 988-994.

[3]A new replication method for fabricating hierarchical polymer surfaces with robust superhydrophobicity and highly improved Oleophobicity Mengying Long, Shan Peng*, Jiaqi Chen, Xiaojun Yang, Wenli Deng. *Colloids and Surfaces A: Physicochem. Eng. Aspects* 507 (2016) 7-17.

[4] Intraocular Lens – Scientific Figure on Research Gate. Available from: https://www.researchgate.net/figure/Contact-angles-of-water-on-hydrophobic-and-hydrophilic-surfaces-a-Contact-angle-is-90_fig1_342344662 [accessed 15 May, 2023].

[5]Analogies to demonstrate the effect of roughness on surface wettability – Scientific Figure on Research Gate. Available from: https://www.researchgate.net/figure/Contact-angle-in-the-Wenzel-model_fig2_320364971 [accessed 15 May, 2023].

[6]Physics of Solid-Liquid Interfaces: From the Young Equation to the Superhydrophobicity – Scientific Figure on Research Gate. Available from: https://www.researchgate.net/figure/Scheme-illustrating-the-Young-equation-The-triad-of-surface-tensions-SL-SA_fig1_304742905 [accessed 15 May, 2023]

Chapter 2

2.1 Literature Survey –



[01] Sanjay et al. and its team found that the Novel and Facile Approach to Prepare Self-cleaning yellow superhydrophobic polycarbonate by simple nitric acid treatment to attain yellow colour polycarbonate (PC) and subsequent surface silylation by Methyltrichlorosilane (MTCS) for superhydrophobicity. A colour of PC can be controlled from light to dark yellow by simply varying the immersion time in nitric acid. The surface silylation by MTCS provides morphologies from nanofibers to nanospheres depending on reaction times. To achieve superhydrophobicity on yellow coloured PC with water contact angle higher than 155° and sliding angle less than 8° . After several water jet impact tests (oblique to vertical angle), no loss in superhydrophobic behaviour was observed confirming its mechanical stability.

[02] PanPan et al. and its team found that the fabrication of microcavity-array superhydrophobic surfaces using an improved template method. In this study, they successfully fabricated polydimethylsiloxane (PDMS) SH micro cavity-array surfaces via a facile and universal method. The SH surface was prepared using an improved template method (ITM) with taro leaves as the template. As is well known, water droplets can freely roll on taro surfaces without leaving any trace of beads. Studies of taro surfaces have revealed that they have a high CA of $\sim 159^\circ$ and a low sliding angle of $\sim 3^\circ$. The CA of the PDMS Negative replica is about 144° . It should be noted that the drop deposited on the negative PDMS replica collapsed after 20 s, and the CA eventually decreased to 152° .

An SH surface is obtained using an ITM. The micro cavity-array surfaces with hierarchical structures are prepared by dip-coating PODS onto PDMS negative replicas. It is found that the fine-scale roughness helped in converting the metastable wetting state into the Cassie state on a concave surface. Our results illustrated the preparation of negative replicas with superhydrophobicity using an ITM and provided a new method for replicating natural leaves. They Fabricated the first superhydrophobic (SH) surface with microcavities, using a simple process. The process included an improved template method (ITM) for constructing the SH surface with cavities, using taro leaves as a pattern mask, and a dip-coating method for modifying the SH surface. The results obtained using the ITM are significantly better than those achieved using traditional template methods. In addition, the water-repellence of the microcavities surface was significantly enhanced by decorating with a layer of polymerized n-octadecylsiloxane nanosheets



[03] Sharad et al. and its team found that the Superhydrophobic microtextured polycarbonate surfaces. A novel approach for fabrication of superhydrophobic polycarbonate (PC) surfaces has been developed based on purely physical process. The water droplet beads up on the microtextured PC in a Cassie–Baxter state exhibiting superhydrophobic nature of the surface. Average height of the micro-pillars formed on replicated PC surfaces played a crucial role in governing the superhydrophobic properties of the resulting microtextured surfaces. The water contact angle could be tailored over a wide range, from 82° for smooth PC surface to 155° , with an increase in average height of the micro-pillars from $1.34\ \mu\text{m}$ to $6.68\ \mu\text{m}$. The infrared (IR) spectroscopy analysis revealed that the PC surface does not undergo any chemical change during thermal replication and further implied that the resulting superhydrophobic behavior was solely due to the physical modification of the surface.

[04] Peng et al. and its team found that the superhydrophobic/electrothermal synergistically anti-icing strategy based on graphene composite. Surface icing tends to cause serious problems such as flash over and the following blackout accident. Although electrothermal system is the most widely used method, how to solve the re-freeze problem as the melted ice tends to stay on the surface is still a challenge. Here, they introduced a superhydrophobic/electrothermal synergistically anti-icing strategy based on graphene composite. To enhance the durability of superhydrophobic surface, the hierarchical structure constructed by the tri-scale nature of inorganic fillers (graphene, carbon nanotubes and silica nanoparticles). Then the hierarchical structure was partially embedded into the substrate by a dissolution and resolidification method. The coupling effect of partially-embedded structure and hierarchical structure led to the superior robustness, which could withstand sandpaper abrasion (500 g load, 8.00 m), the attack of various corrosive liquids, and low/high temperature treatment without losing superhydrophobicity. More remarkably, this graphene superhydrophobic composite retained deicing property even after 30 icing/deicing cycles.

[05] Raad et al. and its team found that the novel approach to fabricating a stable superhydrophobic PC using a phase separation method and selecting a solvent/non-solvent without requiring any surface chemical modification and high chemical stability was proposed in this paper. A systematic study of the dependence of surface morphology on the acetone/DMF solvent mixture treatment was conducted. Resulting surfaces demonstrated that the water CA of the superhydrophobic PC



surface was $160 \pm 2^\circ$. FESEM showed that the surface structure comprised branches or petals outside the 'plant seabeds', which have microflowers that offer nanoscaled roughness on the surface with a hierarchical micro-/nano-binary formation. All samples were maintained at $10\text{--}40^\circ\text{C}$ in ambient atmosphere for 5 h to 4 months to test the stability of the surface. The CAs were measured for each condition with very little change observed. In addition, the PC surface remained superhydrophobic without any contamination after water was sprayed on it.

[06] PanPan Peng, Qingping Ke, Gen Zhou, Tiandi Tang found that superhydrophobic (SH) surface with microcavities, using a simple process. The process included an improved template method (ITM) for constructing the SH surface with cavities, using taro leaves as a pattern mask, and a dip-coating method for modifying the SH surface. The results obtained using the ITM are significantly better than those achieved using traditional template methods.

In addition, the water-repellence of the microcavities surface was significantly enhanced by decorating with a layer of polymerized n-octadecylsiloxane nanosheets.

[07] Steven M. Hurst a, et al shows that, cheap and effective process universally applicable to fabricate superhydrophobic surfaces on various polymers. The process combines sanding and reactive ion etching treatment of the polymer surface to generate respective micro and nanoscale surface roughness, which is followed by subsequent coating of a fluorinated silane molecule to modify the surface chemistry. A 5 min reactive ion etching treatment after sanding is sufficient achieve nanoscale roughness required for superhydrophobic surfaces.

Similar results are obtained with different polymers such as poly(methylmethacrylate) (PMMA), polycarbonate (PC) and cyclo-olefin copolymer (COC), indicating that the process can be applied for creating superhydrophobic surfaces on general polymer substrates..

[08] Khosrow et al summarizes that recent advances in the polymer molding processes used to fabricate superhydrophobic materials. Here, we review replication methods and the materials that can be used by these approaches. They also evaluate the advantages and disadvantages of these methods and discuss the challenges of molding and demolding single-level structures and multilevel structures, with a focus on superhydrophobic surfaces. We evaluate the relationship between structure geometry and the wettability of a surface, highlighting the effect of structure type and size in achieving the desired wettability. We then offer perspectives, discuss current



limitations, and suggest required studies. This review aims to assist researchers in understanding the fundamentals related to the fabrication of patterned surfaces via polymer molding processes and offer avenues for the successful creation of superhydrophobic polymeric surfaces.

[09] Clayton W. Schultz, et al describes that benchtop protocol to create superhydrophobic polydimethylsiloxane (PDMS) via nano contact molding of polycarbonate (PC) that was crystallized by controlled solvent treatment. The crystallized PC chains rearrange into a network of spherulites (spherical semicrystalline domains); the overall surface is rough on the micrometer-scale, while the spherulites themselves consist of nanoscale features. It was confirmed via conventional spectroscopic and high-resolution microscopic investigation that such hierarchical roughness is key to the development of superhydrophobic PC and the substantial enhancement upon PDMS molding. Thus, the prepared PDMS surface has excellent superhydrophobicity with an optimized contact angle of $172 \pm 1^\circ$ and a sliding angle of $<1^\circ$.

[10] Yongquan Qing et al found that an ingenious two-step fabrication of a robust FTPSS with multiple functionalities using a fluorinated inorganic/organic film filled into the concave-convex microstructures of sandpaper matrix was demonstrated. The micro/nano hierarchical structure, in conjunction with the low surface energy imparted by the fluorinated nanoparticles, yielded FTPSS with CA of 160.6 and SA of 3.9. Furthermore, the FTPSS could be used on any substrates at a large scale using double-sided adhesive or glue. Moreover, the surface wettability could be effectively controlled by varying the number of meshes of the sandpaper template.

[11] Stephan Milles et al found that contribution, the self-cleaning efficiency of Al surfaces structured with direct laser writing (DLW), direct laser interference patterning (DLIP) and a combination of both technologies was quantitatively determined. This was performed by developing a characterization method, where the treated samples are firstly covered with either MnO₂ or polyamide micro-particles, then tilted by 15° and 30° and finally washed applying

Up to nine water droplets (10 μ l) over the contaminated surfaces. Then, an optical analysis by image processing of the remaining contamination particles on the textured surfaces was realized after each droplet rolled over the surface. The DLIP textures showed the best performance, allowing the removal of more than 90% of the particles after just three droplets were released. High-speed videos and scanning electron microscopy characterization allowed a deeper



understanding on the cleaning behavior and on the relationship between surface microstructure and particle size and shape.

[12]Mengying Lon et al and its team found that the a new replication method for fabricating hierarchical polymer surfaces with robust superhydrophobicity and highly improved Oleophobicity. In this paper, we reported a very interesting replication method to fabricate various kinds of chemically stable and mechanically durable superhydrophobic and highly oleophobic polymer surfaces by using hierarchical aluminum (H-Al) as the template. It is believed that this work provides a simple replicating method to create hierarchical polymer surfaces ,and then further realize superhydrophobicity and oleophobicity. Specially, the excellent stability and durability of the resultant surfaces are believed to find promising outdoor applications. When coated with PDES, the final hierarchical polymer surfaces showed excellents superhydrophobicity and much improved oleophobicity to hexadecane. Most importantly, these polymer duplicates with coating displayed outstanding chemical stability and excellent mechanical durability.



References-

[01] Ruimin Xing, Sanjay S. Latthe , A. K. Bhosale, Rui Li ,A.Madhan Kumar , Shanhu Liu“A Novel and Facile approach to Prepare Self-cleaning Yellow Superhydrophobic Polycarbonates”

S0167-7322(17)32793-9 DOI: doi:10.1016/j.molliq.2017.10.028

[02] PanPan Peng, Qingping Ke, Gen Zhou, Tiandi Tang “ Fabrication of microcavity-array superhydrophobic surfaces using an improved template method” Journal of Colloid and Interface Science 395 (2013) 326–328. <http://dx.doi.org/10.1016/j.jcis.2012.12.036>

[03]Sharad D. Bhagat, Mool C. Gupta “Superhydrophobic microtextured polycarbonate surfaces” Surface Coatings Technology 270 (2015) 117–122
[.http://dx.doi.org/10.1016/j.surfcoat.2015.03.013](http://dx.doi.org/10.1016/j.surfcoat.2015.03.013)

[04]Peng Wang a , Tao Yao a,b, Ziqiang Li a, Weidong Wei a, Qing Xie c, Wei Duan a, Huilong Han a “A superhydrophobic/electrothermal synergistically anti-icing strategy based on graphene composite” Composites Science and Technology 198 (2020) 108307.
<https://doi.org/10.1016/j.compscitech.2020.108>

[05]Raad S. Sabry and Muntazer I. Al-Mosawi “Novel approach to fabricate a stable superhydrophobic polycarbonate” <http://dx.doi.org/10.1080/02670844.2016.1270620>

[07] Steven M. Hurst a,1, Bahador Farshchiana,1, Junseo Choi a, Jinsoo Kimb., Sunggook Parka, “A universally applicable method for fabricating superhydrophobic Polymer surfaces”



Colloids and Surfaces A: Physicochem. Eng. Aspects 407 (2012) 85–90.

<http://dx.doi.org/10.1016/j.colsurfa.2012.05.012>

[08] Khosrow Maghsoudi, Elham Vazirinasab, Gelareh Momen, and Reza Jafari "Advances in the Fabrication of Superhydrophobic Polymeric surfaces by Polymer Molding Processes" 2020, 59, 9343–9363. <https://dx.doi.org/10.1021/acs.iecr.0c00508>

[09] Steven M. Hurst a,1, Bahador Farshchiana,1, Junseo Choi a, Jinsoo Kimb., Sunggook Parka, A universally applicable method for fabricating superhydrophobic polymer surfaces Colloids and Surfaces A: Physicochem. Eng. Aspects 407 (2012) 85–90 dx.doi.org/10.1016/

[10] Khosrow Maghsoudi, Elham Vazirinasab, Gelareh Momen, and Reza Jafari Advances in the Fabrication of Superhydrophobic Polymeric Surfaces by Polymer Molding Processes 2020, 59, 9343–9363 dx.doi.org/10.1021/

[11] Clayton W. Schultz, Cliff L. W. Ng, and Hua-Zhong Yu Superhydrophobic Polydimethylsiloxane via Nanocontact Molding of Solvent Crystallized Polycarbonate: Optimized Fabrication, Mechanistic Investigation, and Application Potential 2020, 12, 3161–3170 DOI: 10.1021

[11]. Yongquan Qing, Cai Long, Kai An a, Chuanbo Hu, Changsheng Liu Sandpaper as template for a robust superhydrophobic surface with self-cleaning and anti-snow/icing performances Journal of Colloid and Interface Science 548 (2019) 224–232 doi.org/10.1016/j

[12] Stephan Millesa, Marcos Solderaa, Thomas Kuntzec, Andrés Fabián Lasagnia, Characterization of self-cleaning properties on superhydrophobic aluminum surfaces fabricated by



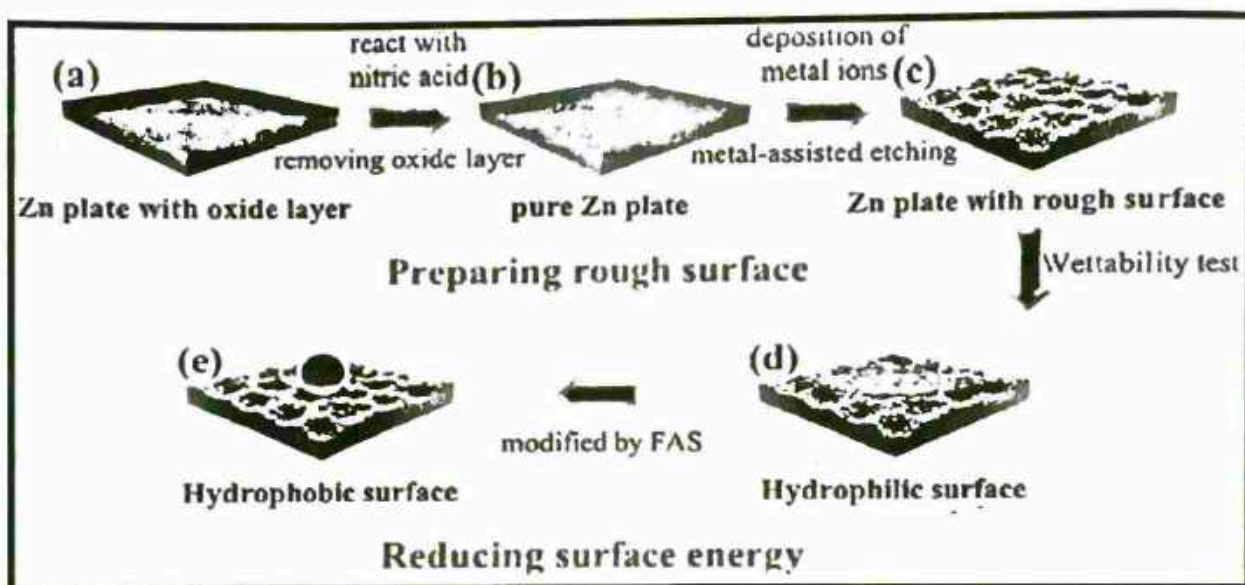
2.2 Fabrication Techniques/ Methods

Fabrication of super-hydrophobic surfaces usually requires the roughening of surface to get micro-nanostructures followed by surface modification which leads to low surface energy. Some methods like chemical etching, solution-immersion process, spray coating use coating material for surface modification after surface roughening, while some methods like laser electrodeposition, template deposition do not need to modify the surface. Simplicity, least time consumption, cost-effectiveness and versatility are the important parameters during fabrication process. Moreover, characteristics like durability, corrosion resistance and storability of super-hydrophobic surfaces formed are achieved at different levels from each method.

2.2.1 Chemical etching



Developed physically and thermally stable SHS by a simple and cost-saving method. Chemical etching method was used for developing micro-nanostructures on the surface of Al alloy which was used as a substrate. After surface roughing of substrate with abrasive paper and ultrasonically cleaning with deionized water, it was treated with NaOH first and then with solution of HCl and CH₃COOH resulting in micro-nanostructures on surface. Then surface energy of etched substrate was lowered by immersing it in the solution of silanes. The maximum water contact angle (WCA) obtained was 165° and contact angle hysteresis (CAH) was 3°. SHS formed remained stable after different tests and was storable for more than a month. developed a rapid fabrication method of SHS.



Metal-assisted chemical etching was done on zinc plate which was used as substrate. Pure zinc plate was first ultrasonically cleaned and dried in oven

Chu and Wu fabricated SHS on Al and Cu substrates simultaneously using chemical etching method. Surfaces were first cleaned and then solution of HCl and Cu(NO₃)₂ was used for Al plate etching, while for copper plate etching, solution of HNO₃ and AgNO₃ was used. Surface modification was done using aqueous solution of FAS. The results showed that for Al and Cu substrates, the micro-nanostructures were similar to that of lotus leaves and moss, respectively. The WCA was found to be 164 ± 1° for Al and 157 ± 1° for Cu. The measured rolling angles were 2 ± 1° and 6 ± 1° for Al and Cu, respectively. Moreover, condensation experiment was also performed over both SHS resulting in lower droplet density, higher droplet jumping probability, slower droplet growth rate and lower surface coverage for Al as compared to Cu. Yin et al.



developed SHS using chemical etching method. Al plate was used as the substrate material. For etching process, a solution of HF and HCl in deionized water was prepared. Later, Al substrate was immersed in that solution for roughing the surface. For surface modification, three different coatings such as perfluoroalkyltriethoxysilane (PFO), PA and room temperature vulcanized (RTV) coating were separately used to determine the super-hydrophobic nature of surfaces. WCA measurements showed the maximum CA of 162, 161.7 and 158.3° for PFO, PA and RTV coatings, respectively. Environmental factors varied, that is, temperature in range of -10 to 30°C and RH values of 30, 60 and 90%, during condensation experiment to determine any changes in super-hydrophobic nature of surfaces. CA, SA and contact area fraction were calculated and it was found that with increasing RH and lowering temperature, CA and SA values decreased and increased, respectively, while contact area fraction increased showing increase in wettability. Super-hydrophobicity of RTV coating was greatly affected during condensation at low temperature which was recovered simply by drying.

2.2.3 Solution immersion

A simple one-step method of SHS fabrication. Solution-immersion process was used in which copper foams were used as substrate. Pure copper foams after properly washed, ultrasonically cleaned and dried were immersed in ethanolic stearic acid solution for 4 h, 2 days and 4 days. With increase in immersion time, clusters formed became denser, covered the surface more, the skeleton of 3D porous structure got thicker and rougher while pore size decreased. WCA kept increasing

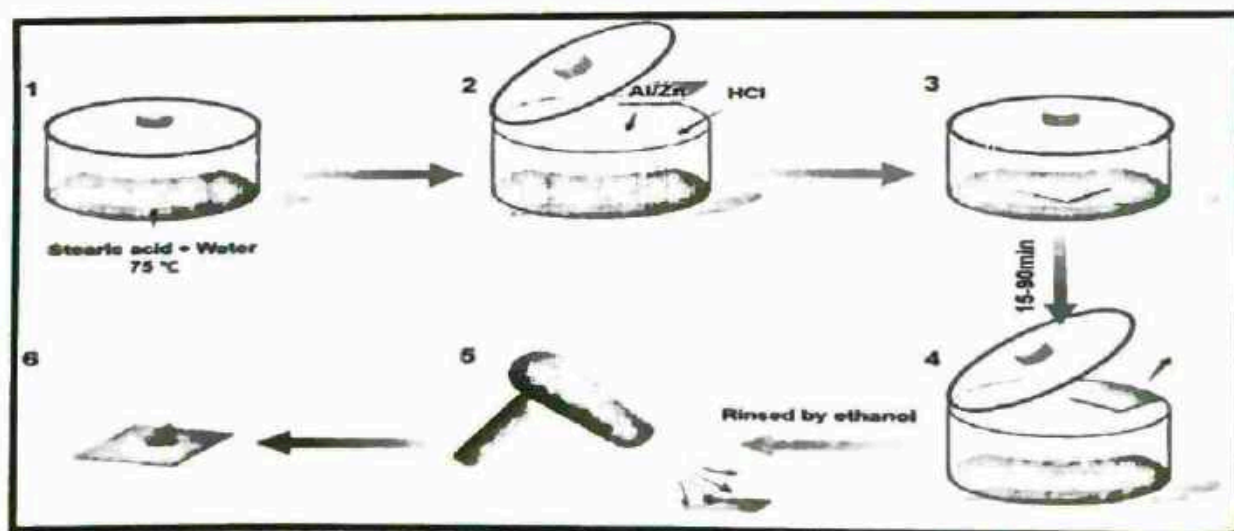


Fig. Solution immersion



With immersion time to 156° for 4 days and SA decreased to minimum of 4° . This fabrication process resulted in robust and mechanically stable SHS. Zhao et al. developed a simple and pure chemical approach of fabricating SHS. SiO_2 -coated SiC nanowires were used as substrate material which already contained nanostructures on surface. Fabrication process started with the preparation of ethanol solution of FAS. The substrate was then immersed in the solution for a day which resulted in the surface with super-hydrophobic nature. The treatment process did not produce any change in the surface morphology, micro-texture and crystal phase of substrate. WCA of $5 \mu\text{m}$ droplet was measured to be 153° . To check for durability, SHS fabricated was irradiated by UV lamps of 100 W which resulted in the great durability of surface. Zheng et al. fabricated SHS on glass substrate by dip coating sol-gel process. At first, glass plate was properly washed and cleaned. Then, two solutions named as 'A' and 'B' were first prepared. Solution 'A' contained glycidoxypopyl trimethoxysilane (GPTS) modified with silica sol while solution 'B' consisted of PTFE emulsion. Both solutions were mixed into each other. After then, glass was immersed in the mixture by dip-coating process. Later, drying and heating of modified glass resulted in SHS. Both micro and nanostructures were produced on surface and WCA and SA were found to be 156 and 6° , respectively. Weight contents of SiO_2 and PTFE were also varied and then optimized to be 20:9. To check the thermal stability of coating, the temperature of reacting process varied as 100, 200, 250 and 300°C . Best super-hydrophobic features were found at 250°C after which WCA and SA kept decreasing and increasing, respectively. Fabrication procedure used was very simple and of low cost.

2.2.4 Laser electrodeposition

Laser electrodeposited composite method to fabricate SHS. Copper channel was used as substrate. First surface was roughed by laser, then electrodeposition was performed to obtain microstructures on surface and then dried. No coating material was used for lowering surface energy. Static WCA was found to be decreasing by increasing the channel width and the maximum WCA was 156° . Rolling angle was also determined and it was less than 5° . Moreover, the effect of microstructures on pressure drop was also studied. Pressure drop increased with increase in channel width and was also smaller in super-hydrophobic channel as compared to smooth channel. Friction factor was reduced in super-hydrophobic micro-channels by maximum of 48.8%. Li et al. used a new one-step and simple idea for the fabrication of super-hydrophobic and hydrophobic



surfaces. Zinc sheets were used as a substrate material. Laser ablation process was used to increase surface roughness of zinc sheet dipped in aqueous solution of H_2O_2 . Two types of laser ablation were used in the study such as nanosecond (ns) and femtosecond (fs) laser ablation. ZnO and $Zn(OH)_2$ were generated on the zinc surface as a result of laser ablation. Both types of laser ablation created different microstructures on surface. Clustered flower-like microstructures were formed on ns-laser ablated sample while non-directional flaky nanostructures were formed on fs-laser ablated sample. Roughness was also found to be higher for ns-laser ablated sample due to which it was super-hydrophobic with WCA and WSA of 158.5 and 4.3° , respectively. On the other hand, fs-laser ablated sample was highly hydrophobic with WCA of 145.7° and WSA of 12.5° .

Developed fabrication method of SHS on copper substrate and the focus of this study was kept to the fast fabrication of SHS. First, copper substrate was exposed to the nanosecond laser beam originating from laser beam machining of 3.3 watt power and 20 Hz frequency. Earlier before this study, it had already been found that laser beam produced layer of CuO on sample which was hydrophilic and it took a long time about 27 days to be converted into SHS which had Cu_2O on the surface. So, instead of keeping the laser textured surface in ambient conditions, it was made super-hydrophobic using annealing at low temperature, that is, $100^\circ C$. This accelerated the conversion of CuO into Cu_2O resulting in the formation of SHS after 13 h. As copper is also stable with ethanol, so additional reduction in time to get SHS was achieved when ethanol was used by which SHS was formed in less than 5 h. WCA was also found to be maximum of 165° showing super-hydrophobicity.

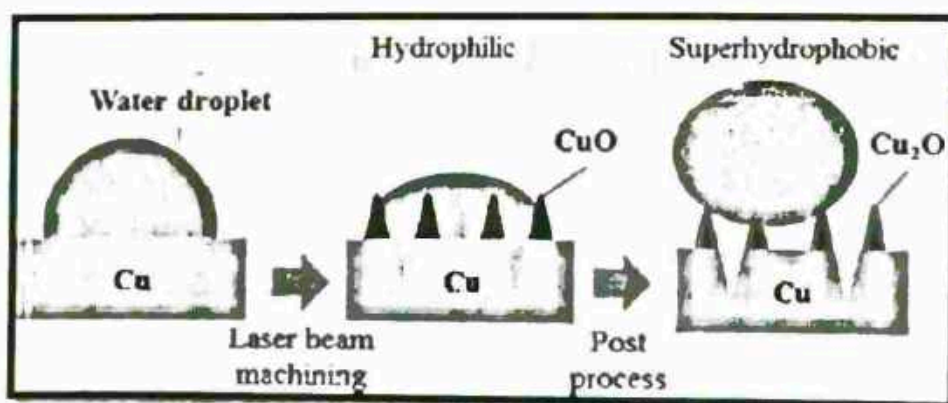


Figure 4. Schematic illustration of SHS with laser beam machining and post-process [24]



2.2.5 Template method-

Template deposition method for the fabrication of SHS using copper sheet as substrate. The fabrication method consisted of three steps. First step was to prepare template from polystyrene microspheres powders. Second step was to put copper plate in polystyrene colloidal microspheres with CuSO_4 solution as an electrolyte. The electrodeposition potential was about -0.5 V and SEM images were taken after deposition time of 19 s. During this process, copper atoms filled the voids in the template. In final step, surface was modified using fluorosilane solution resulting in a SHS. WCA of $5 \mu\text{L}$ droplet was measured to be 156.3° . WCA increased with increase in deposition time to 19 s and then decreased after that. Bhagat and Gupta developed a purely physical process of fabricating super-hydrophobic polycarbonate surfaces (PC). Silicon wafers were used as substrate which along-with PC were initially washed and cleaned properly. In first step of fabrication, micro-textures were produced on substrate by high power laser and in second step, those microstructures were thermally replicated on PC surface by sandwiching them between two hot plates having different temperatures. Upon cooling, both surfaces were then separated from each other. Effect of replication temperature was such that when temperature varied from 155 to 175°C , micro-pillars formed on PC surface varying in the average height from $1.34 \mu\text{m}$ to $6.68 \mu\text{m}$. During this, WCA also varied from 82° to maximum 155° . Super-hydrophobic PDMS surfaces were also fabricated by this process with maximum CA of 162° . This physical process of fabrication resulted in robust SHS with good mechanical properties.



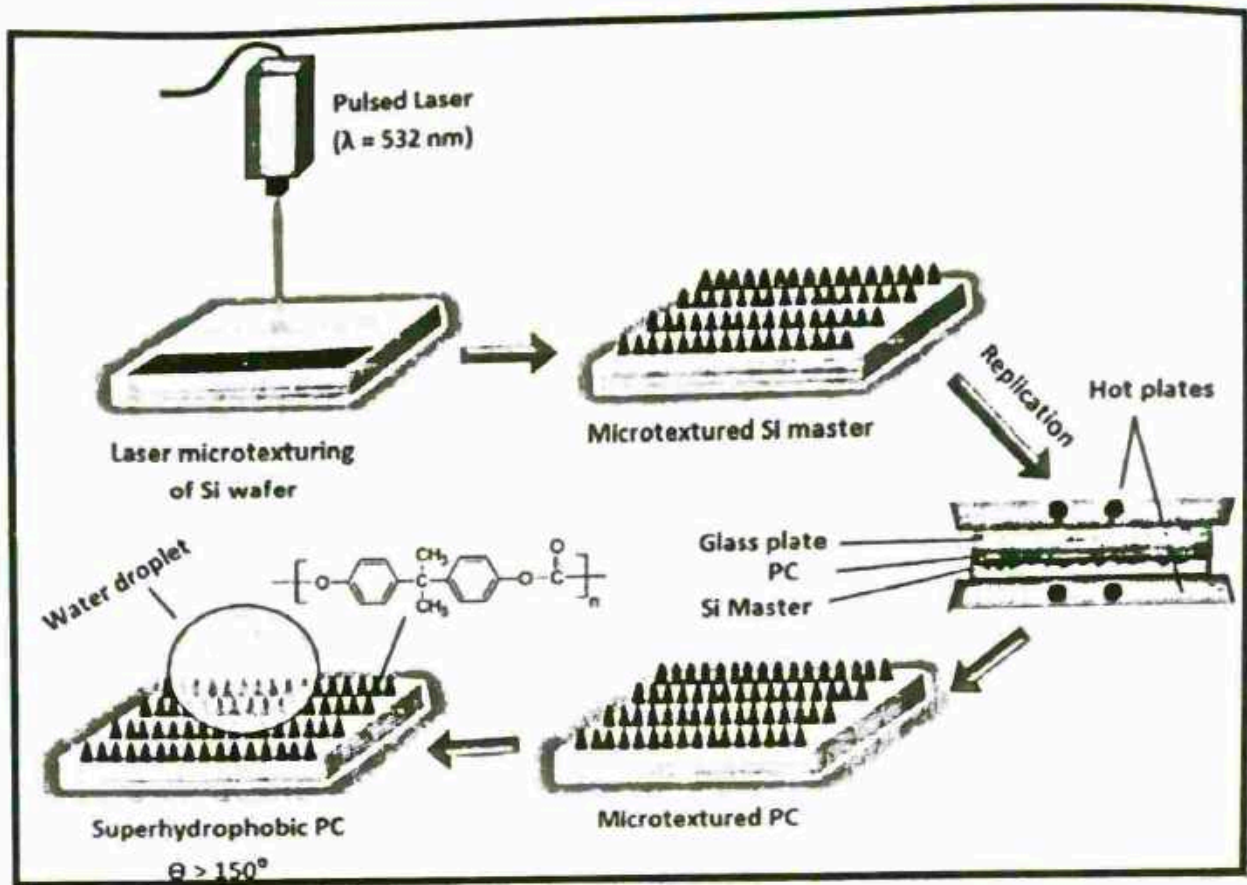
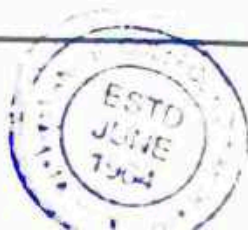


Figure 2.4.5 Schematic diagram for fabrication of super-hydrophobic PC by laser micro-texturing of Si wafer and its subsequent replication [26].

2.2.5 .Spray coating

Momen and Farzaneh fabricated exceptionally stable SHS using a simple and cost-effective approach of spray coating. Glass substrate used was first ultrasonically cleaned followed by preparation of three separate samples. First sample 'a' consisted of RTV silicon rubber (SR) in hexane, sample 'b' of ZnO nanoparticles in hexane and SR while sample 'c' contained both ZnO and SiO₂ nanoparticles in hexane and SR. Then all three samples were separately spray-coated on glass slides by using spray gun. SEM investigations showed that sample 'a' coating resulted in smooth surface. Sample 'b' coating caused nan-scale roughness on surface while sample 'c'



coating resulted in both micro and nanostructures. WCAs for all samples a, b and c were measured to be 117.3, 132.5 and 162.7°, respectively. Different stability tests carried out on SHS resulted in slight decrease in WCA after 10 days by immersing in different pH solutions. UV and humidity had also little effect on WCA. Against heating treatment at 150°C for almost a month, WCA was decreased just a little showing the stability of SHS. Ipekci et al. developed one-step spray-coating method of fabricating SHS which had improved mechanical robustness and durability. A matrix was required for better dispersing of silica nanoparticles functionalized with fluorinated silanes. Hydroxyl-terminated polystyrene was used as a matrix which reacted with substrate to form polymer brushes through covalent bonding. Glass slides were used as a substrate. WCA measurements showed that CA was greater than 170° and SA was approaching 0°. WCA was highest for weight-ratio of 1 between PS-OH and FNP. Effect of curing temperature was also determined and WCA was found to be maximum at 190°C. Abrasion tests also showed that WCA decreased after grain velocity of 10 km/h. SHS formed were also transparent to 85%. Enhancement of mechanical robustness was different for different substrates and polymers.

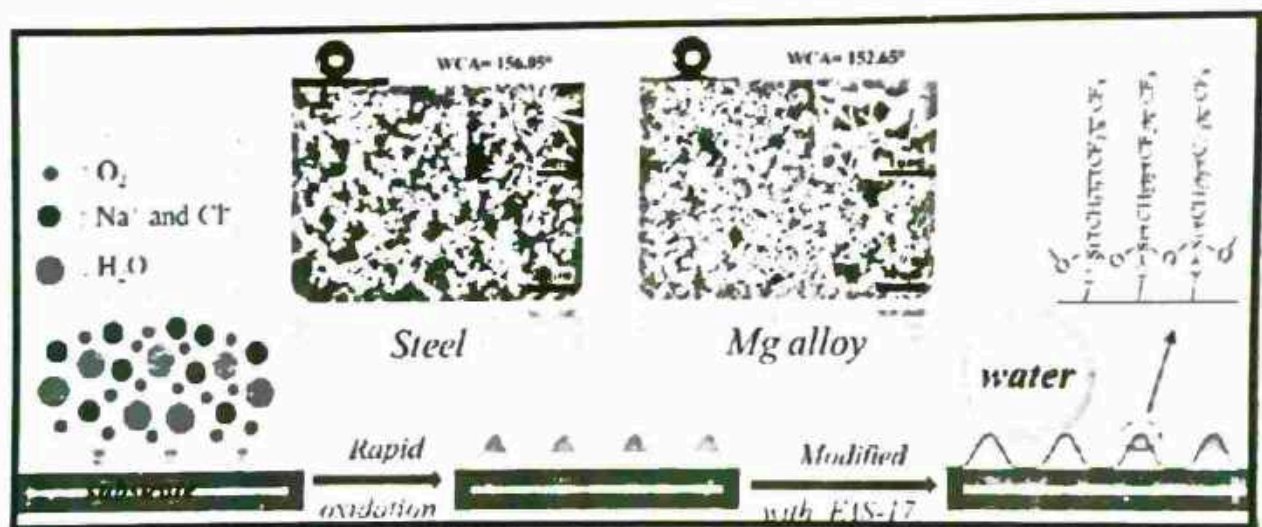


Figure 6. Schematic diagram for fabrication of SHS by salt-spray method [30].



References

1. https://en.wikipedia.org/wiki/Lotus_effect [Accessed: 22-11-2017]
2. Darmanin T, Guittard F. Superhydrophobic and superoleophobic properties in nature. *Biochemical Pharmacology*. 2015;18:273-285. DOI: 10.1016/j.mattod.2015.01.001
3. Esmailirad A, Rukosuyev MV, Jun MBG, van Veggel FCJM. A cost-effective method to create physically and thermally stable and storable super-hydrophobic aluminum alloy surfaces. *Surface & Coatings Technology*. 2016;285:227-234. DOI: 10.1016/j.surfcoat.2015.11.023
4. Qi Y, Cui Z, Liang B, Parnas RS, Houfang L. A fast method to fabricate superhydrophobic surfaces on zinc substrate with ion assisted chemical etching. *Applied Surface Science*. 2014;305:716-724. DOI: 10.1016/j.apsusc.2014.03.183
5. Chu F, Xiaomin W. Fabrication and condensation characteristics of metallic superhydrophobic surface with hierarchical micro-nano structures. *Applied Surface Science*. 2016;371:322-328. DOI: 10.1016/j.apsusc.2016.02.208
6. Yin L, Wang Y, Ding J, Wang Q, Chen Q. Water condensation on superhydrophobic aluminum surfaces with different low-surface-energy coatings. *Applied Surface Science*. 2011;258:4063-4068. DOI: 10.1016/j.apsusc.2011.12.100
7. Liao R, Zuo Z, Guo C, Yuan Y, Zhuang A. Fabrication of superhydrophobic surface on aluminum by continuous chemical etching and its anti-icing property. *Applied Surface Science*. 2014;317:701-709. DOI: 10.1016/j.apsusc.2014.08.187



8. Nguyen TPN, Dufour R, Thomy V, Senez V, Boukherroub R, Collinier Y. Fabrication of superhydrophobic and highly oleophobic silicon-based surfaces via electrolyses etching method. *Applied Surface Science*. 2014;295:38-43. DOI: 10.1016/j.apsusc.2013.12.166.

3.2 Characterization technique-

3.2.1 Scanning Electron Microscopy (SEM)

The scanning electron microscope (SEM) uses a focused beam of high-energy electrons to generate a variety of signals at the surface of solid specimens. The signals that derive from electron-sample interactions reveal information about the sample including external morphology (texture), chemical composition, and crystalline structure and orientation of materials making up the sample. In most applications, data are collected over a selected area of the surface of the sample, and a 2-dimensional image is generated that displays spatial variations in these properties. Areas ranging from approximately 1 cm to 5 microns in width can be imaged in a scanning mode using conventional SEM techniques (magnification ranging from 20X to approximately 30,000X, spatial resolution of 50 to 100 nm). The SEM is also capable of performing analyses of selected point locations on the sample; this approach is especially useful in qualitatively or semi-quantitatively determining chemical compositions (using EDS), crystalline structure, and crystal orientations (using EBSD). The design and function of the SEM is very similar to the EPMA and considerable overlap in capabilities exists between the two instruments.

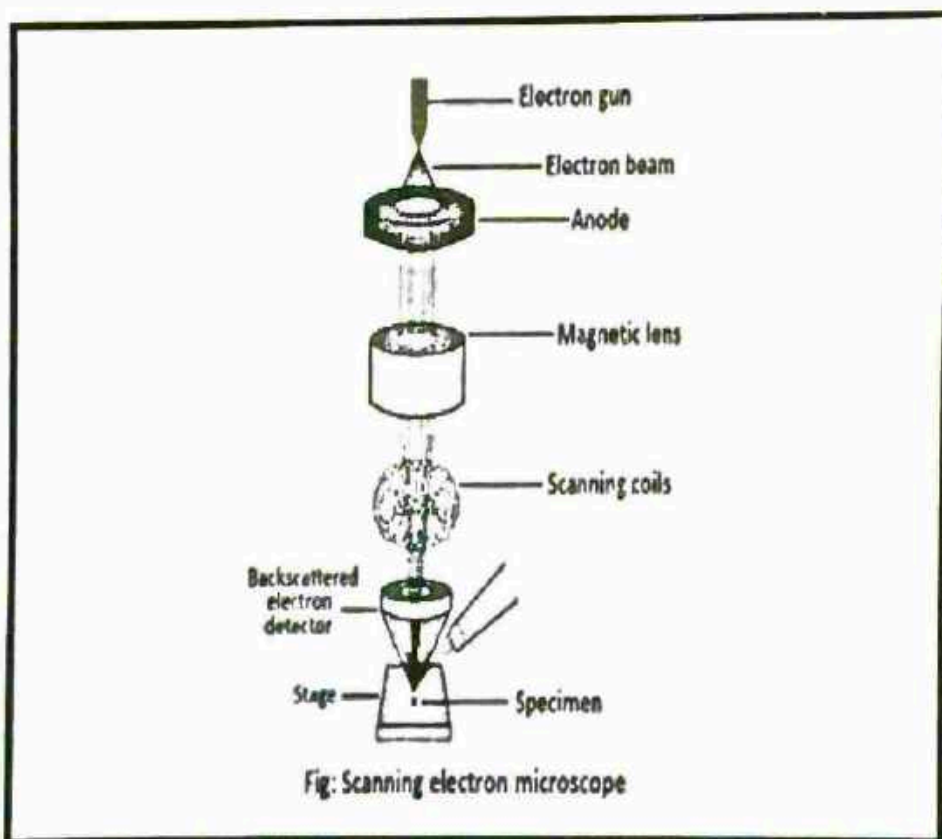
- **Fundamental Principles of Scanning Electron Microscopy (SEM)**

Accelerated electrons in an SEM carry significant amounts of kinetic energy, and this energy is dissipated as a variety of signals produced by electron-sample interactions when the incident electrons are decelerated in the solid sample. These signals include secondary electrons (that produce SEM images), backscattered electrons (BSE), diffracted backscattered electrons (EBSD that are used to determine crystal structures and orientations of minerals), photons (characteristic X-rays that are used for elemental analysis and continuum X-rays), visible light (cathodoluminescence—CL), and heat. Secondary electrons and backscattered electrons are



commonly used for imaging samples: secondary electrons are most valuable for showing morphology and topography on samples and backscattered electrons are most valuable for illustrating contrasts in composition in multiphase samples (i.e. for rapid phase discrimination). X-ray generation is produced by inelastic collisions of the incident electrons with electrons in discrete orbitals (shells) of atoms in the sample. As the excited electrons return to lower energy states, they yield X-rays that are of a fixed wavelength (that is related to the difference in energy levels of electrons in different shells for a given element). Thus, characteristic X-rays are produced for each element in a mineral that is "excited" by the electron beam. SEM analysis is considered to be "non-destructive"; that is, x-rays generated by electron interactions do not lead to volume loss of the sample, so it is possible to analyze the same materials repeatedly.

- Scanning Electron Microscopy (SEM) Instrumentation – How Does It Work?



Essential components of all SEMs include the following:

- Electron Source ("Gun")
- Electron Lenses
- Sample Stage
- Detectors for all signals of interest
- Display / Data output devices
- Infrastructure Requirements:
 - Power Supply
 - Vacuum System
 - Cooling system
 - Vibration-free floor
 - Room free of ambient magnetic and electric fields

SEMs always have at least one detector (usually a secondary electron detector), and most have additional detectors. The specific capabilities of a particular instrument are critically dependent on which detectors it accommodates.

Applications

The SEM is routinely used to generate high-resolution images of shapes of objects (SEI) and to show spatial variations in chemical compositions: 1) acquiring elemental maps or spot chemical analyses using EDS, 2) discrimination of phases based on mean atomic number (commonly related to relative density) using BSE, and 3) compositional maps based on differences in trace element "activators" (typically transition metal and Rare Earth elements) using CL. The SEM is also widely used to identify phases based on qualitative chemical analysis and/or crystalline structure. Precise measurement of very small features and objects down to 50 nm in size is also accomplished using the SEM. Backscattered electron images (BSE) can be used for rapid discrimination of phases in multiphase samples. SEMs equipped with diffracted backscattered electron detectors (EBSD) can be used to examine microfabric and crystallographic orientation in many materials.

3.2.2 Atomic Force Microscopy

Atomic force microscopy (AFM) or scanning force microscopy (SFM) is a very-high-resolution type of scanning probe microscopy (SPM), with demonstrated resolution on the order of fractions of a nanometer, more than 1000 times better than the optical diffraction limit. Atomic



force microscopy[1] (AFM) is a type of scanning probe microscopy (SPM), with demonstrated resolution on the order of fractions of a nanometer, more than 1000 times better than the optical diffraction limit. The information is gathered by “feeling” or “touching” the surface with a mechanical probe. Piezoelectric elements that facilitate tiny but accurate and precise movements on (electronic) command enable precise scanning. Despite the name, the Atomic Force Microscope does not use the Nuclear force.

History

The AFM was invented by IBM scientists in 1985.[6] The precursor to the AFM, the scanning tunneling microscope (STM), was developed by Gerd Binnig and Heinrich Rohrer in the early 1980s at IBM Research – Zurich, a development that earned them the 1986 Nobel Prize for Physics. Binnig invented[5] the atomic force microscope and the first experimental implementation was made by Binnig, Quate and Gerber in 1986.

The first commercially available atomic force microscope was Introduced in 1989. The AFM is one of the foremost tools for imaging, measuring, and manipulating matter at the nanoscale.

Applications-

The AFM has been applied to problems in a wide range of disciplines of the natural sciences, including solid-state physics, semiconductor science and technology, molecular engineering, polymer chemistry and physics, surface chemistry, molecular biology, cell biology, and medicine. Applications in the field of solid state physics include (a) the identification of atoms at a surface, (b) the evaluation of interactions between a specific atom and its neighboring atoms, and (c) the study of changes in physical properties arising from changes in an atomic arrangement through atomic manipulation.

In molecular biology, AFM can be used to study the structure and mechanical properties of protein complexes and assemblies. For example, AFM has been used to image microtubules and measure their stiffness.

In cellular biology, AFM can be used to attempt to distinguish cancer cells and normal cells based on a hardness of cells, and to evaluate interactions between a specific cell and its neighboring



cells in a competitive culture system. AFM can also be used to indent cells, to study how they regulate the stiffness or shape of the cell membrane or wall.

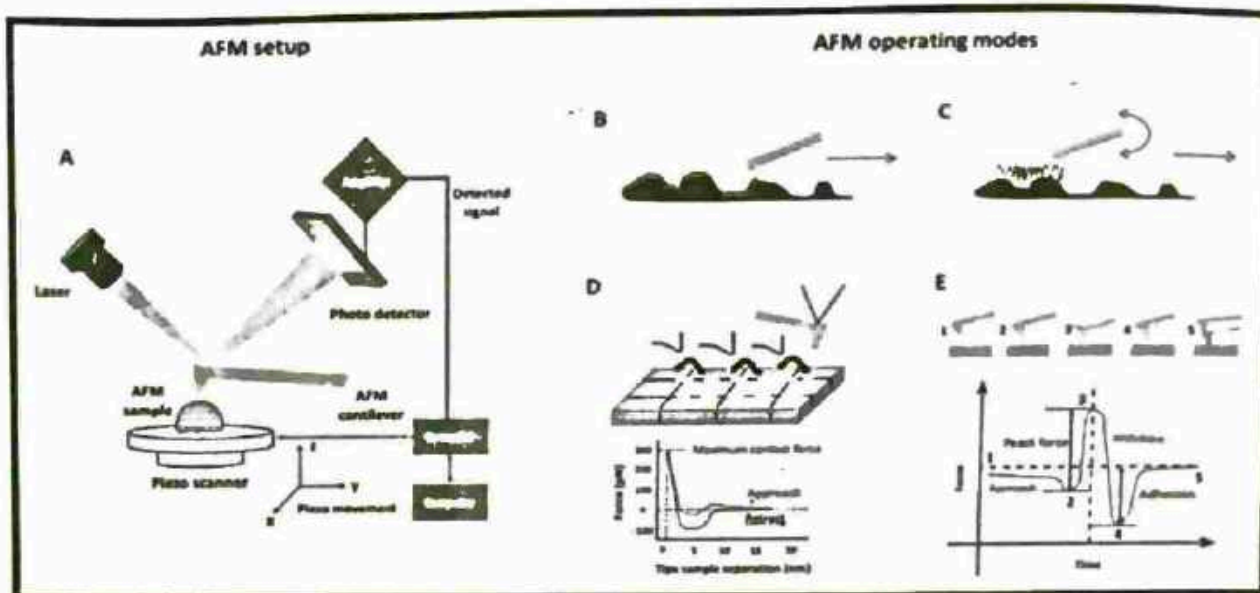


Figure -An atomic force microscope on the left with controlling computer on the right

AFM microscopes are among the best solutions for measuring the nanoscale surface metrology and material properties of samples. A conventional compound light microscope is limited to a maximum sample magnification of approximately 1000x; a quantity that is dictated by the wavelengths of visible light. This provides a resolution of approximately 0.2 micrometers (μm), which means it is impossible to distinguish two points that are closer together than around 200 nanometers (nm). The limitations of this resolving power have become painfully evident in recent decades, particularly since the genesis of advanced technologies like the scanning electron microscopy (SEM) and atomic force microscopy (AFM).

AFM microscopes are based on a unique non-optical surface interrogation technique. This is built on the fundamentals of scanning probe microscopy, which utilizes a physical probe to measure the surface features of samples with atomic resolution for lateral and height measurements.

3.3.3 FTIR :



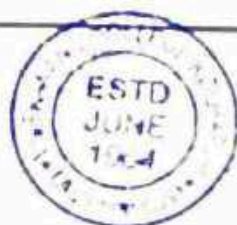
Fourier Transform Infrared Spectroscopy, also known as FTIR Analysis or FTIR Spectroscopy, is an analytical technique used to identify organic, polymeric, and, in some cases, inorganic materials. The FTIR analysis method uses infrared light to scan test samples and observe chemical properties.

Working :

The FTIR instrument sends infrared radiation of about 10,000 to 100 cm^{-1} through a sample, with some radiation absorbed and some passed through. The absorbed radiation is converted into rotational and/or vibrational energy by the sample molecules. The resulting signal at the detector presents as a spectrum, typically from 4000 cm^{-1} to 400 cm^{-1} , representing a molecular fingerprint of the sample. Each molecule or chemical structure will produce a unique spectral fingerprint, making FTIR analysis a great tool for chemical identification.

What is FTIR used for?

FTIR spectroscopy is an established technique for quality control when evaluating industrially manufactured material, and can often serve as the first step in the material analysis process. A change in the characteristic pattern of absorption bands clearly indicates a change in the composition of the material or the presence of contamination. If problems with the product are identified by visual inspection, the origin is typically determined by FTIR microanalysis. This technique is useful for analyzing the chemical composition of smaller particles, typically 10 -50 microns, as well as larger areas on the surface. FTIR analysis is used to Identify and characterize unknown materials (e.g., films, solids, powders, or liquids), Identify contamination on or in a material (e.g., particles, fibers, powders, or liquids), Identify additives after extraction from a polymer matrix, Identify oxidation, decomposition, or uncured monomers in failure analysis investigations.



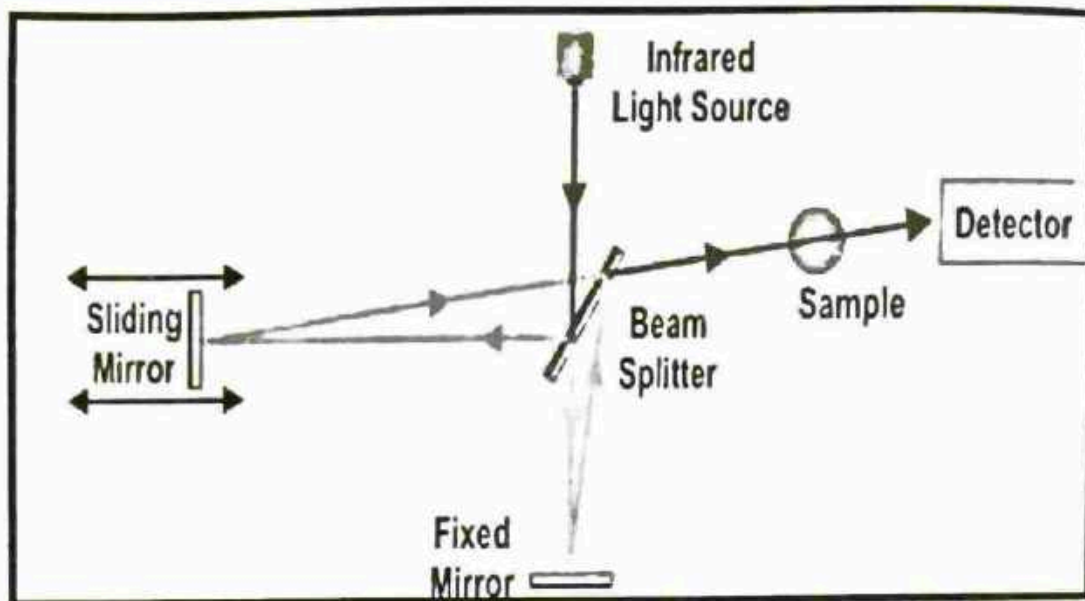


Figure 3.3.3 Fourier transform infrared spectroscopy



References-

1. https://serc.carleton.edu/research_education/geochemsheets/techniques/SEM.html

2. <https://rtilab.com/techniques/ftiranalysis/#:~:text=Fourier%20Transform%20Infrared%20Spectroscopy%2C%20also,samples%20and%20observe%20chemical%20properties.>

3. https://www.researchgate.net/publication/228370294_Atomic_force_microscopy_AFM_Basics_and_its_important_applications_for_polymer_characterization_An_overv



Chapter 3

3.1 Introduction –

The template method is a common method to obtain superhydrophobic surfaces. This method focuses on obtaining superhydrophobicity by replicating the rough structure on the surface of a template with low surface energy. The templates can be divided into “soft templates” and “hard templates” according to the materials used. The research of the template method is mainly divided into two approaches: In the first, the artificial substrate is formed by etching and other methods, and then a variety of required superhydrophobic structures are obtained by soft-template curing and hard-template imprinting. In the other, the “hard template” method is improved so that it can be applied to a variety of hard templates, and the template is in the superhydrophobic state with a contact angle higher than 150° . The substrates used are divided into two types: natural substrates and artificial substrates. Natural substrates include lotus leaves, petals, and other superhydrophobic texture structures, whereas artificial substrates include microstructures formed through etching and other methods.

The replication of natural substrates by the template method is the main way to achieve a superhydrophobic surface, from natural to artificial, and is an important means to study their biological superhydrophobic properties. Hong et al. [64] replicated the functional nanometer patterns of cicada wings by the “hard template method”, first by thermal embossing onto PVC polymer to form a mirror-image template, followed by deposition, activation, and photolithographic curing of the resin to replicate the cicada wing structure onto a glass plate. The surface contact angle obtained by this method was about 132° , which was higher than that of the PVC polymer at 86° . Sun et al. [53] used the soft template method to cast polydimethylsiloxane (PDMS) onto a lotus leaf and isolated it after curing a “mirror image template”. The PDMS was then used to cast the “mirror image template” again, and trimethylchlorosilane (TMCS) was used as an anti-adhesive between the two templates to replicate the lotus leaf structure on PDMS, which had a similar surface contact angle to the lotus leaf at 160° .

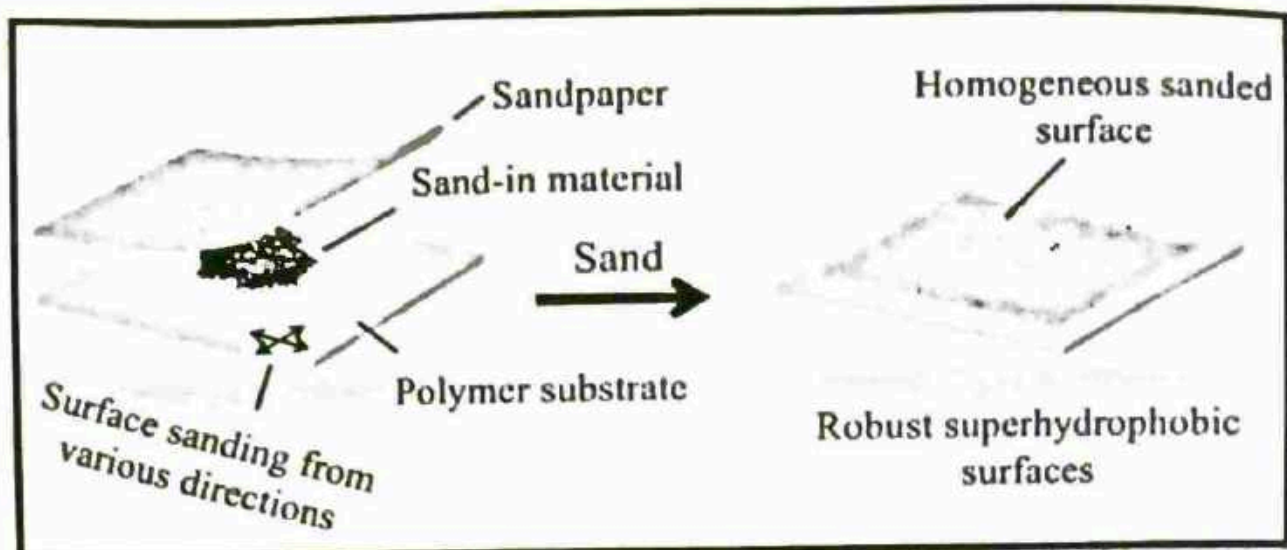


Figure 3.1 template method

3.2 Experimental

3.2.1 Materials-

Sand papers(60,180,320,220 grit etc.) were purchased from chemical agent and also polycarbonate substrate were purchased from chemical agent.

3.2.2 Fabrication of superhydrophobic sand paper surfaces-

- Firstly, the maintain the temperature of hot plate adjusting by knob.
- After take a hot plate then put polycarbonate substrate on it and on the surface of polycarbonate substrate such as 60 grit, 180 grit etc.
- Apply pressure on it with the help of weight like as 1000 gm, 5000 gm etc. Overall, this process is carried out by 3-4 hours .After switch off the button and check the superhydrophobicity of polycarbonate substrate by putting water droplet on the surface of polycarbonate substrate.



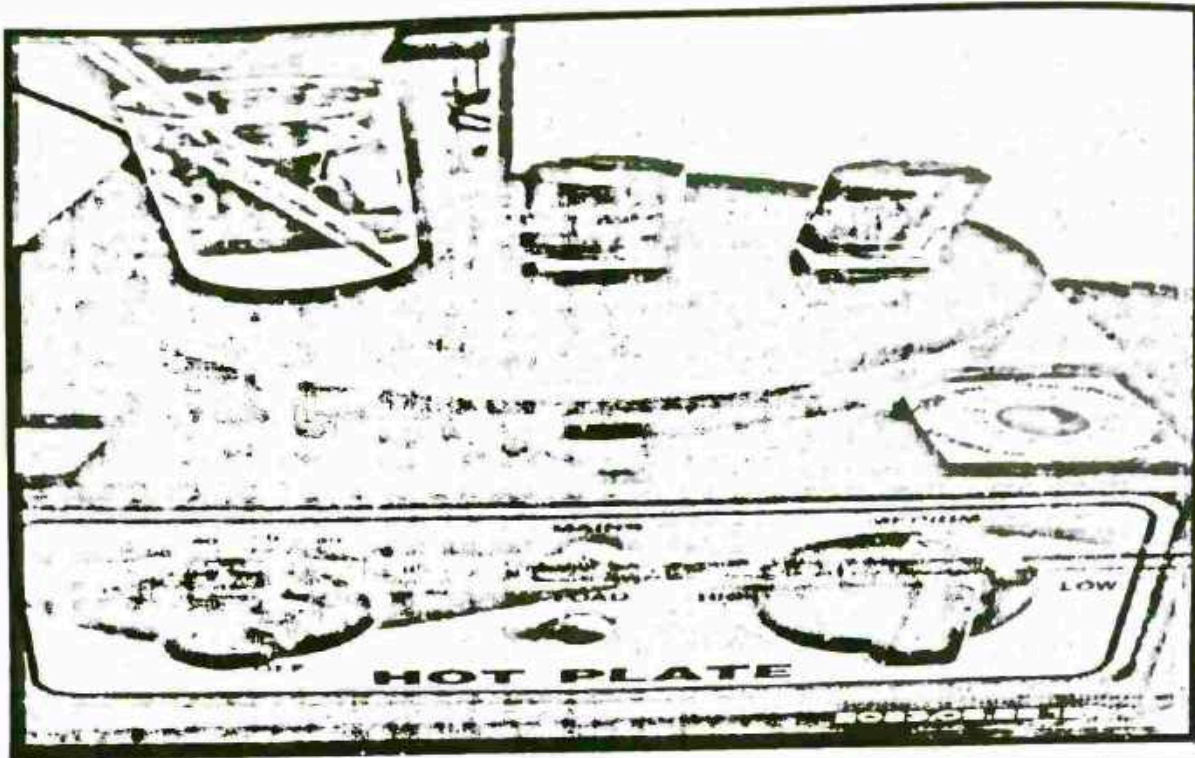


Figure 3.2.1 – Experimental Set up

3.3 Characterization-

The surface morphology of the sample (polycarbonate substrate) were investigated by Scanning Electron Microscopy (SEM). The surface roughness, contact angle, sliding angle of water droplet and oil droplet can be measured by Scanning Electron Microscopy.

The following SEM figure shows contact angle of water droplet on the surface of polycarbonate substrate.



Left Angle: 93.384120609645
Right Angle: 104.310279390355

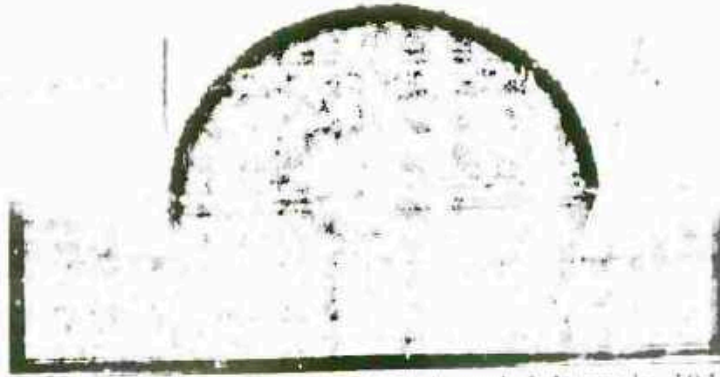


Fig.(a). Image shows left angle -90.384° and right angle -104.31°

Left Angle: 93.831963379535
Right Angle: 100.032133197231



Fig.(b). Image shows left angle -93.83° and right angle -100.03°



Left Angle: 92.687713211605
Right Angle: 101.150444094128



Fig.(c). Image shows left angle -92.68° and right angle -101.15°

Left Angle: 91.1534504511064
Right Angle: 97.6189611791108



Fig.(d). Image shows left angle -91.15° and right angle -97.69°



3.4 Result and discussion –

The different contact angle for different samples were observed on the surface of polycarbonate substrate after the given temperature of hot plate at various time.

The detailed analysis of this samples was made with the aid of morphology studies.

Surface morphology, surface roughness and water Contact angle of the sample –

A superhydrophobicity can be achieved by nano fibrous structure which provides high surface area or high aspects ratio which is very useful for the formation of air pocket. The trapped air pocket in the fibrous structure can be minimized the solid-liquid interaction performing the superhydrophobicity state(Cassie-Baxter Wetting) state.

At the time of 2 hour , it shown in wide gaps with surface roughness $1.65\mu\text{m}$. However, for other polycarbonate substrate for different time, polycarbonate substrate of surface existed with continuous increasing roughness of $0.641\mu\text{m}$, $0.649\mu\text{m}$, $0.759\mu\text{m}$, $1.573\mu\text{m}$ for respective polycarbonate substrate.

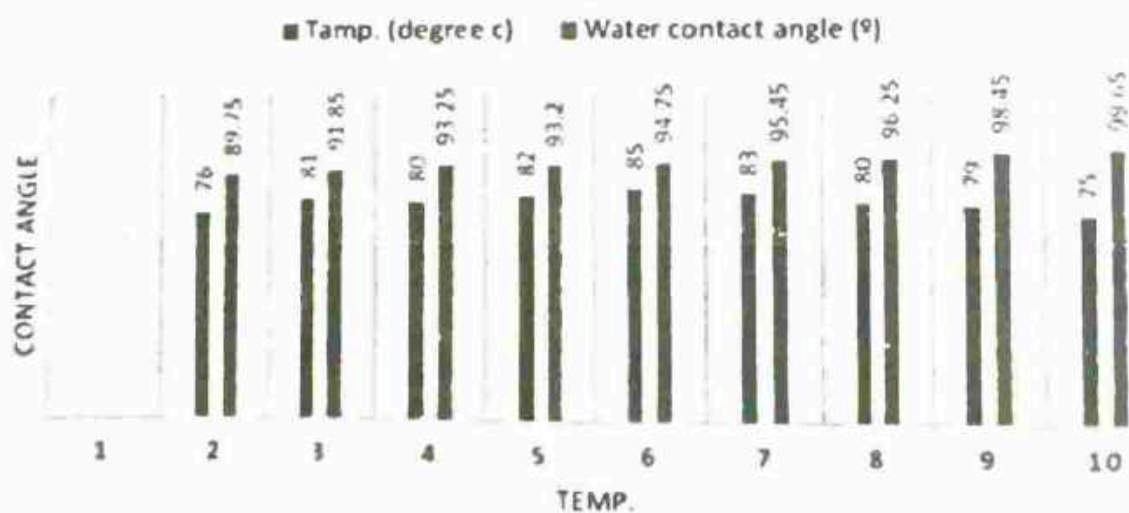
The contact angle of polycarbonate substrate 91.85° at temperature 81°C , 93.25° at temperature 80°C , 99.65° at temperature 75°C for respective sand papers of 60 grit, 80 grit and 320 grit.

This surface shows hydrophobicity of polycarbonate substrate with the help of water droplet.



Table 1- study of surface morphology

Sample (grift)	Water contact angle (°)	Water sliding angle (°)	Tamp. (degree c)	Roughness in μm	UV illumination				WCA (°) (After 01 Adhesive tape cycle)
					15 min	30 min	45 min	60 min	
180	89.75	-	76	0.649	96.9	81.2	89.9	82.0	-
60	91.85	-	81	0.572	95.9	-	83.6	84.9	-
80	93.25	-	80	1.812	103	-	71.8	69.1	
180	93.2	-	82	0.759	49.8	82.8	70.8	63.6	-
320	94.75	-	85	1.573	93.2	57.9	84.2	65.8	C
100	95.45	-	83	0.641	94.3	90.1	78.9	89.9	80.2
220	96.25	-	80	1.86	125	73.4	84.2		86.6
100-c	98.45	-	79	1.651	90.3	91.9	91.1	90.7	88.4
320	99.65	-	75	0.453	75.8	-	88	88.2	86.5



Chapter 4

4.1 Conclusion-

In conclusion, we fabricated a unique rough polycarbonate substrate by a template method by using sand papers to fabricated surface morphology of the sample. The as prepared rough polycarbonate substrate becomes hydrophobic it modified using sand paper , and its average contact angle is 99° . This method is very simple and easy provides a unique surface morphology of the sample.

A polycarbonate is attracting the attention of many materials scientists due to its low cost mechanical stability and high visible light transparency apart from costly physical methods. We used simple and cost effective chemical method to achieve superhydrophobicity of polycarbonate substrate for self-cleaning application. The self-cleaning superhydrophobic polycarbonate can be extensively used in daily life such as door and window glasses, wind shields of vehicles, solar panel and many.

Since the superhydrophobic materials have been found to be great application value in the field of anti-icing, various methods have been successfully developed to prepare superhydrophobic coating morphology plays a crucial role in liquid solid phase transformation for controlling ice nucleation and crystallization significantly.

Researcher should develop superhydrophobic anti icing coating that are easy and rapid to prepare on a large scale, low cost, non- toxic to humans and environmental friendly. This are also urgent problems

That extremely expected finally it is work that even though a long period of time will be spend to achieve the extensive application of superhydrophobic coating in our daily life and industrial applications.

4.2 Future Plan-



In future, we will check modified sample by the use of Scanning Electron Microscopy (SEM), Atomic force Microscopy (AFM), Fourier Transform Infra-red Microscopy (FTIR).

